Diploma Thesis

Optimisation of a temperature swing adsorption for synthesis gas purification

Carried out for the purpose of obtaining the degree of Master of Science (MSc or Dipl.-Ing or DI), submitted at TU Wien, Faculty of Technical Chemistry, by

Tobias BOLEK, BSc

Mat.Nr.: 0925215

under the supervision of

Univ.Prof. Dipl.-Ing. Dr.techn. Hermann Hofbauer

Institute for Process Engineering, Environmental Technology and Technical Biosciences

reviewed by

Dipl.-Ing. Jürgen Loipersböck

Institute for Process Engineering, Environmental Technology and Technical Biosciences

Getreidemarkt 9, 1060 Wien

This work was supported by BEST – Bioenergy and Sustainable Technologies GmbH.

I confirm that going to press this thesis needs the confirmation of the examination committee.

Affidavit

I declare in lieu of oath, that I wrote this thesis and performed the associated research myself, using only literature cited in this volume. If text passages from sources are used literally, they are marked as such.

I confirm that this work is original and has not been submitted elsewhere for any examination, nor is it currently under consideration for a thesis elsewhere.

Vienna, July 2020 _____

Signature

Acknowledgements

I would like to thank Univ.Prof. Dipl.-Ing. Dr.techn. Hermann Hofbauer for the opportunity to write my diploma thesis at the Institute for Process Engineering, Environmental Technology and Technical Biosciences.

Special thanks go to my supervisor Dipl.-Ing. Jürgen Loipersböck. Only with his help and support it was possible for me to carry out the necessary experiments and write this thesis. I thank him for all the time, patience and support he gave me.

Furthermore, I would like to thank my family and my girlfriend who have always been there for me in the last years and supported me during my studies, at any time.

Abstract

The gasification of biogenic residual material is an important contribution to the non-fossil production of chemicals. During gasification, beside the product gas, dust, higher hydrocarbons (tars) and sulphur compounds which must be removed before usage in a synthesis plant, are generated.

To remove tars to synthesis gas standard efficiently, two-stage gas cleaning has been developed. In the first step, high-molecular tar components are separated in a scrubber. In the second step, low-molecular tar components (e.g. benzene, toluene, xylene) are adsorbed in an adsorption plant on activated carbon. As a result, a high purified synthesis gas originates which can be used for various synthesis applications. To operate this gas cleaning efficiently, the activated carbon must be regenerated. In a laboratory scale unit model tars are adsorbed and desorbed on activated carbon. Due to parameter variation of desorption temperature, desorption time and amount of flushing gas the process is optimised. Furthermore, possible displacement effects of the separate tar components are investigated.

Kurzfassung

Die Vergasung von biogenen Reststoffen stellt einen wichtigen Beitrag zur nichtfossilen Produktion von Chemikalien dar. Während der Vergasung entstehen, neben dem Produktgas, Staub sowie höhere Kohlenwasserstoffe (Teere) und Schwefelverbindungen, welche vor dem Einsatz in einer Syntheseanlage entfernt werden müssen.

Um Teere effizient auf Synthesegasstandard zu reinigen wurde eine zweistufige Gasreinigung entwickelt. Im ersten Schritt werden hochmolekulare Teerkomponenten in einem Wäscher abgeschieden. Die niedermolekularen Teerkomponenten (z.B.: Benzol, Toluol, Xylol) werden in einer Adsorptionsanlage an Aktivkohle adsorbiert (zweiter Schritt). Somit entsteht ein hochreines Synthesegas, welches für diverse Syntheseanwendungen verwendet werden kann.

Um diese Gasreinigung effizient betreiben zu können, muss die Aktivkohle regeneriert werden. In einer Laboranlage sollen Modellteere an Aktivkohle adsorbiert und desorbiert werden. Durch eine Parametervariation von Desorptionstemperatur, Desorptionszeit und der Spülgasmenge soll der Prozess optimiert werden. Weiters sollen mögliche Verdrängungseffekte der einzelnen Teerkomponenten untersucht werden.

Table of contents

1. Introduction

Crude oil is of great importance for the chemical industry. It serves as a starting material for numerous products such as plastics, paints or cleaning agents. Due to the challenges that have arisen in recent years and need to be solved, be it global environmental pollution, climate change or the general shortage of resources, it is necessary to move away from the intensive use of fossil raw materials.

The key to a sustainable future for the chemical industry is therefore renewable carbon. There are three possible sources for this: [1, 2]

1. Recycling - There is enormous potential for chemical and mechanical recycling in the chemical industry

2. Direct use of carbon dioxide as a raw material

3. Biomass (is dealt with in this thesis)

Europe, in particular, is dependent on imports of raw materials, especially oil and gas, and is surrendering to the ever-increasing competition on the world market. The resource-efficient and sustainable use of biogenic raw materials therefore offers the economy an alternative that can be used in several ways. [1, 2]

1.1 Aim of the work

During the gasification of biomass and biogenic residues, for the production of synthesis gas, hydrocarbons are produced. Especially condensable hydrocarbons further referred as tars are problematic. These must be removed, otherwise the gas produced is not pure enough for further use in various synthesis applications. In addition, the separated components can in turn be used as starting material for a wide range of chemical products. The gas is purified by adsorption on activated carbon. Since it is fully loaded after a certain time, it must be regenerated in order to clean the gas efficiently. The aim of this work is to optimise this regeneration process by parameter variation.

1.2 Biomass in the chemical industry

Biomass generally refers to all organic materials of a biogenic, non-fossil nature. This refers to matter living and growing in nature and resulting waste products, both from living and already dead organic mass. [3]

Due to the depletion of fossil resources, a conversion of sources of raw materials to renewable and regenerable ones is a necessary part of the strategy and solution. The material use of biomass products offers numerous advantages, such as the reduction of dependence on fossil raw materials, the conservation of non-renewable resources, the cleanliness of soil, water and air, the biodegradability as well as the reduction of CO_2, further environmental pollution and mountains of waste. [3]

Currently, the share of biomass in organic chemistry in Europe is about 14%. There are significant differences from country to country. For example, the share of renewable raw materials in Denmark is already 40%, whereas in most Eastern European countries it is less than 10%. Overall, however, a slight increase can be observed in recent years. [2]

In principle, the chemical industry has always used renewable raw materials derived from biomass as the basis for many of its products. However, this is mainly because in certain areas they have technical and economic advantages over fossil raw materials and not for ecological reasons. One of the most important advantages is, for example, that nature has already provided a synthesis and produced complex chemical components. This concerns primarily starch, cellulose, sugar, oils and fats as well as active pharmaceutical ingredients which are used for the production of detergents, adhesives, plastics, cosmetics, fibres, paints and even pharmaceuticals. Renewable raw materials are therefore used primarily in the field of specialty chemicals. [4]

Renewable raw materials have so far played a subordinate role in the production of basic chemical building blocks in the field of petrochemicals. However, in those fields where biomass can replace naphtha (= light petroleum fraction obtained from distillation of crude oil; the most important component of the chemical industry), the aforementioned natural synthesis is not desirable. The highly functionalised building blocks provided by nature must be defunctionalised in general in order to be used in chemical production as bio-based platform chemicals (= chemicals that serve as the basis for downstream chemicals, e.g: lactic acid, ethanol, ...) can be used in chemical production. [4]

Since raw materials based on biomass cannot simply be converted in existing conventional plants, research into new and further development of already known processes for the conversion of biomass is necessary, e.g: [5]

- The further development of biological processes (e.g. biosynthesis in the form of starch and cellulose degrading bacteria)
- The combination of substance transformations (e.g. chemical and biotechnological processes)
- The further development of thermal, chemical and mechanical processes [e.g. through new digestion methods, gasification (synthesis gas) and liquefaction of biomass] - This category includes the topic of this thesis

To the last category, precisely gasification, belongs the subject of this work. Therefore, a closer look will be taken at this area.

1.3 Overview of the procedure

During gasification, numerous impurities are produced by side reactions, which need to be removed before the resulting gas can be used in a catalyst-driven synthesis.

A flow scheme of gasifier and coarse gas cleaning, which are part of a biomass gasification plant based on dual fluidised bed technology, is shown in Figure 1.

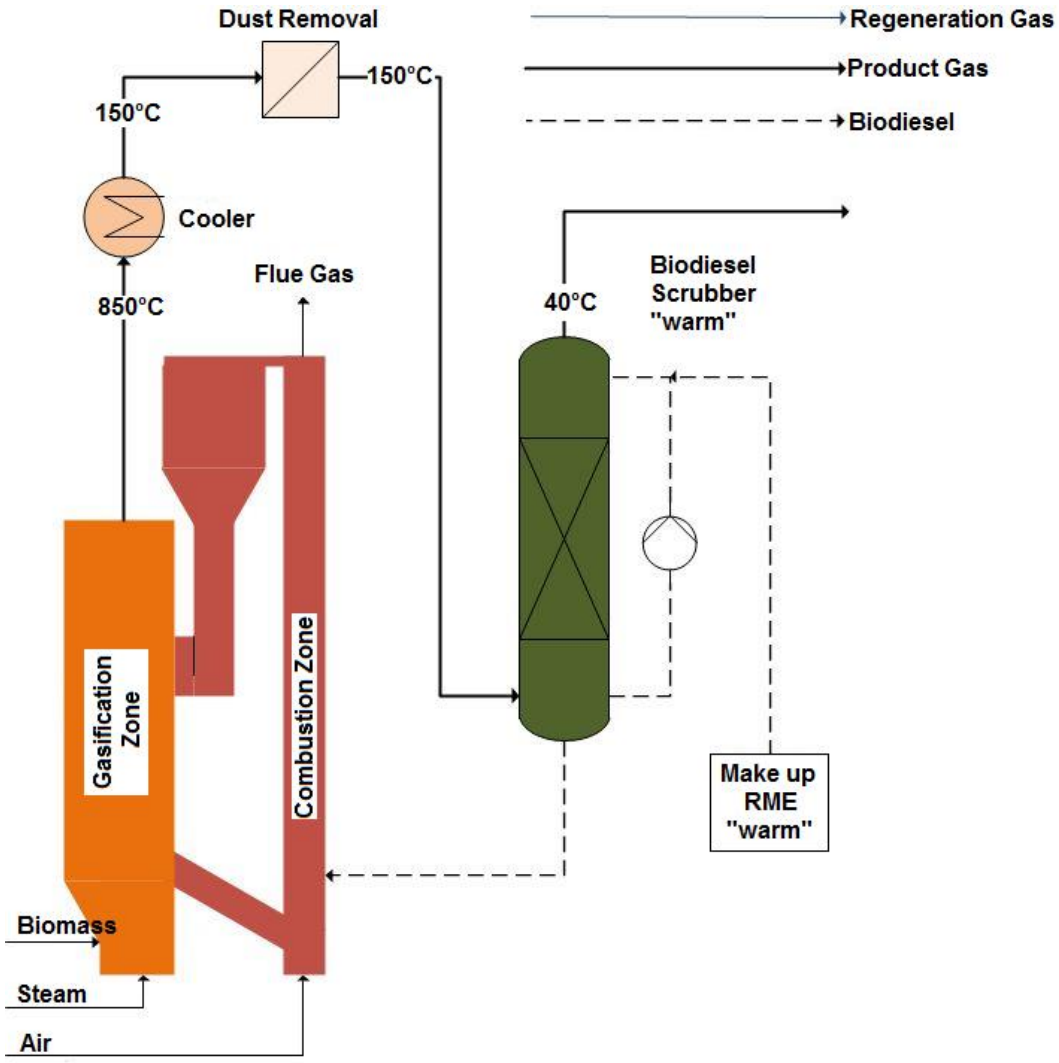

Figure 1: Schematic structure of a dual fluidised bed gasifier with following gas cleaning (adapted from [6])

DFB stands for **d**ual **f**luidised **b**ed. This is an allothermal gasification process in which steam is used as the gasification agent. In this process, two reaction zones [gasification and combustion] are used, which are coupled by a slide and a cyclone. Biomass is gasified in a bubbling bed with steam as gasification and fluidisation agent. In the presence of catalytic active bed material, the added water vapour reacts with the combustibles under heat consumption to form the main gas components hydrogen (H_2), carbon monoxide (CO), carbon dioxide (CO_2) and methane (CH_4). [6]

A slide transports the bed material and the non-gasified biomass into the combustion zone. A fast-fluidised bed is established there by fluidisation with air. The non-gasified biomass is burned and the bed material is reheated. The bed material is separated from the combustion gas stream by a cyclone and is reinjected to the gasification reactor. The resulting gasification product is an almost nitrogen-free gas which is well suited for various synthesis applications, such as Fischer-Tropsch-Synthesis or for methanol production. [6]

However, in order to be used for such applications, impurities must be removed. First the product gas is cooled down and coarser impurities (dust) are removed. Then it is

transferred to a biodiesel scrubber. Here almost all heavy tar components are separated. [6]

However, some volatile hydrocarbons and sulphur components still have to be removed. This is where the experiments of this work start. To separate the above-mentioned substances from the gas, activated carbon is used. However, since this is fully loaded after a certain time, it must be desorbed, i.e. the impurities must be removed from it. This is done according to the principle of temperature swing adsorption. In this process, the temperature is increased, which causes the components to loosen. The higher the temperature, the faster this happens. This process should be optimised by varying the parameters. Thus, on the one hand, a temperature should be found which causes a fast and sufficient release of the impurities and, on the other hand, does not require a too long cooling time. [6, 7]

The following pages provide a brief overview of the state of the art regarding biomass gasification and gas cleaning processes, the most important terms used in this context as well as the description and evaluation of the tests carried out.

2. Theoretical background

The following chapter shows the theoretical background related to this work. At first, biomass gasification is described, especially fluidised bed gasification. Then the production of synthesis gas, the resulting problematic substances and the general gas composition are discussed. Afterwards, an overview of different gas purification processes, especially adsorption, is given. Finally, the gas chromatography used is explained.

2.1 Biomass gasification

In addition to the complete oxidation, i.e. combustion, of a combustible, solid biomass can also be converted into a secondary energy source, which can then be converted into usable energy at another location and at another time in a further step (e.g. production of biomethane). This is possible by gasification. Gasification is the conversion of a solid fuel into a combustible gas by the action of heat and the use of a gasification agent (e.g. air, oxygen or water vapour). The resulting product gas consists mainly of carbon monoxide (CO), carbon dioxide (CO_2), hydrogen (H_2) and methane (CH_4). Its properties depend on the gasification material, gasification agent used and the reaction conditions. In general, the CO content is decisive for its energy content and calorific value. Finally, the gas produced can be decoupled in place and time, used for heat and power generation or as a starting product for further processing (e.g. into fuels). [8]

In principle, the conversion processes in gasification are the same as in combustion. However, the individual steps of the thermo-chemical conversion take place separately. Thus, in contrast to combustion, there is only partial oxidation of the combustible. In a gasification reactor, various chemical reactions take place, mainly endothermic. This means that heat is required to gasify biomass. A distinction is made between autothermal and allothermal gasification. In the autothermal process, the heat is generated in the reactor itself by partial combustion of the biomass via air. In the allothermal process, heat is supplied indirectly, for example via a heat exchanger or a heated, circulating bed material. [8]

However, not only endothermic reactions take place in the gasifier, but also exothermic processes. This process therefore generates heat in addition to the product gas. The product gas consists of a mixture of various gas components, whereby some undesired by-products are also produced. These include long-chain organic compounds known as tars or condensates, as well as dust and ashes. Fuel, type and quantity of the gasification agent, temperature level, pressure and reaction time in the reactor ultimately determine the composition of the product gas. If the product gas is used for syntheses (e.g. methanol synthesis), it is also called synthesis gas. This, as well as the problematic tars, will be discussed in more detail in later chapters. [8, 9]

2.1.1 Stages of thermo-chemical gasification

When biomass is gasified, various physical and chemical processes take place. The design of the reactor, the process control and the catalysts that may be used influence the course of the reactions in different ways. In general, however, the gasification process can be divided into four stages. These are heating and drying, pyrolytic decomposition, oxidation and reduction. Depending on the reactor design, the individual steps run independently of each other or partly in parallel. Figure 2 shows these phases schematically. [8]

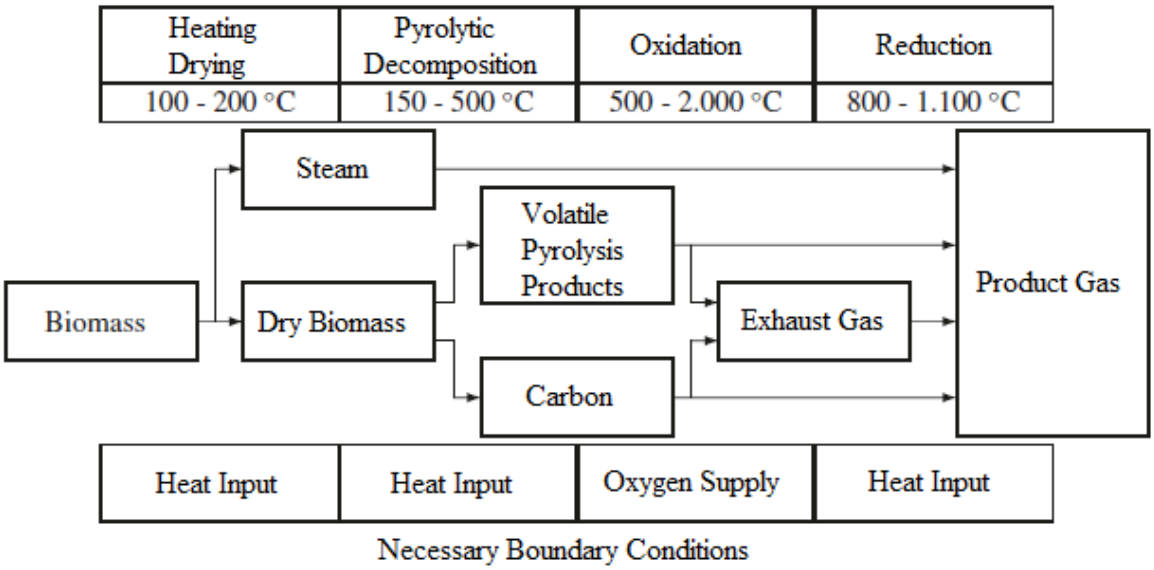

Figure 2 Stages of biomass gasification (adapted from [8])

- Heating and drying: Here the biomass is heated and the remaining water content in the combustible evaporates and is heated at up to 200 °C. [8]

- Pyrolytic decomposition: Pyrolytic decomposition of the macromolecules that are the main molecules of biomass takes place at a temperature between 150 and 500 °C. The effect of heat causes these molecules to break up and takes place almost completely without any oxygen. Gaseous hydrocarbons, pyrolysis oils and pyrolysis coke are formed. What remains is a solid residue consisting mainly of carbon and ash. [8]

- Oxidation: Here the solid, liquid and gaseous products are reacted by further heat and in the presence of a gasification agent. The temperature rises to over 500 °C. The remaining pyrolysis coke is converted into combustible gases. In some cases, carbon is also burned, with the following reactions taking place, among others: [8, 9]

$$C + O_2 \rightarrow CO_2 \qquad \Delta H = -393.5\ \mathrm{kJ/mol} \qquad (2.1)$$

$$C + \frac{1}{2}O_2 \rightarrow CO \qquad \Delta H = -110.5\ \mathrm{kJ/mol} \qquad (2.2)$$

Equations 2.1 and 2.2 show that the complete oxidation of C to CO_2 releases an energy amount of 393 kJ/mol, whereas the CO reaction releases only 110 kJ/mol. This means that about 2/3 of the energy stored in the solid biomass is retained in the gas produced. Therefore, CO formation is particularly important for synthesis gas production. In contrast to combustion, the aim of biomass gasification is to produce as much CO and as little CO_2 as possible.

- Reduction: The main part of the combustible components of the product gas are formed in this process. Carbon dioxide and water are reduced with solid carbon to form carbon monoxide and hydrogen. The following reactions take place primarily: [8]

$$C + CO_2 \rightarrow 2CO \qquad \Delta H = 159.9\ \mathrm{kJ/mol} \qquad (2.3)$$

$$C + H_2O \rightarrow CO + H_2 \qquad \Delta H = 118.5\ \mathrm{kJ/mol} \qquad (2.4)$$

Equation (2.3) is the so-called Boudouard-reaction. Equation (2.4) is called the heterogeneous water-gas reaction. Both are endothermic reactions, which are linked to an increase in volume due to the gas formation that takes place. Heterogeneous means that the reaction partners involved are in different phases. Here, a solid phase (C) reacts with a gas phase (CO_2 or H_2O). In addition to these reactions, also others take place. Particularly worth mentioning are the homogeneous (the reaction partners are present in gaseous form) water-gas-shift-reaction (2.5) and the methanation reaction (2.6), in which carbon and hydrogen are converted to methane: [8]

$$CO + H_2O \rightarrow CO_2 + H_2 \qquad \Delta H = -40.9\ \mathrm{kJ/mol} \qquad (2.5)$$

$$C + 2H_2 \rightarrow CH_4 \qquad \Delta H = -87.5\ \mathrm{kJ/mol} \qquad (2.6)$$

Although the supply with air will burn some of the solid carbon or carbon monoxide, and thus some of the desired products, these reactions are intentional, as they provide the heat required for the entire gasification process. In addition, there are also undesirable reactions that lower the calorific value of the product gas, such as the oxyhydrogen gas reaction (2.7): [8]

$$H_2 + \frac{1}{2}O_2 \rightarrow H_2O \qquad \Delta H = -285.9\ \mathrm{kJ/mol} \qquad (2.7)$$

In addition to temperature and pressure during the gasification process, the choice of the gasification agent also plays a decisive role in the final product gas composition. Table 1 gives an overview of this.

Table 1: Influence of the gasification agent on the composition and energy content of the product gas (adapted from [8])

Gas component in [Vol.-%]	Gasification agent		
	Air	Air / O_2 (80%)	Water vapour
CO	10-20	40-50	25-47
H_2	9-20	9-17	35-50
CH_4	1-8	<1	14-25
CO_2	10-20	19-25	9-15
N_2	40-55	15-30	2-3
Calorific value in [MJ/m^3_{STP}]	4-6.5	7-9	12-17

It is evident that the use of pure oxygen or water vapour massively increases the calorific value of the gas, since no or only little nitrogen, which would be introduced with normal air, hinders the formation of CO and H_2. [8]

However, since the design of the gasification reactor also has an influence on the product gas composition, the following chapter will discuss the different designs. [8, 9]

2.1.2 Types of gasifiers

Basically, the different types of gasifiers can be divided into three groups: Fixed bed gasifiers, fluidised bed gasifiers and entrained flow gasifiers. This classification is based on the fluid dynamic behaviour of the solid material when flowing through the gasification reactor against gravity. A brief overview of the different gasifiers, is given in Figure 3: [9]

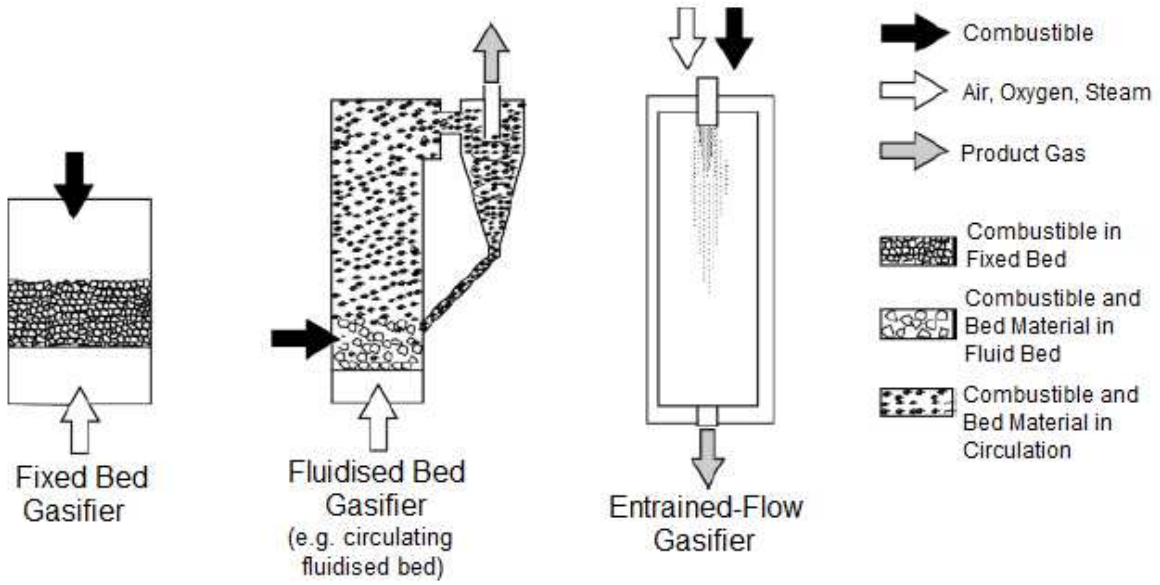

Figure 3: Schematic illustration of different gasification systems with regard to the fluid dynamic behaviour of solids and gas (adapted from [9])

- Fixed bed gasifier: The fuel particles are not moved by the gas flow. This is due to the low flow velocities and/or the large fuel particles. Due to the discharge of the gasification residue in the bottom area of the reactor, the fuel slowly migrates through it in the form of a bulk. Depending on the flow direction of the gas relative to the fuel, a distinction is made between co-current and counter-current gasifiers. [8, 9]

- Fluidised bed gasifier: Here the flow velocity of the gas in the fluidised bed area is already so high that the particles are moved in the reactor. This leads to an excellent mixing of fuel and bed material and a nearly isothermal temperature in the reaction chamber. In contrast to the fixed bed, it is necessary to use bed material with a defined grain size in order to achieve a good fluidised bed condition. If flow velocities are used which do not result in the discharge of bed material, the fluidised bed is stationary. However, if bed material is discharged, this is referred to as a circulating fluidised bed. [8, 9]

- Entrained-flow gasifier: In this type of gasifier, the fuel is normally introduced into the reactor as dust or in paste form through a burner. The gasification reactions take place in a so-called dust cloud. For this reason, the fuel must be treated accordingly before gasification. For example, it must be ground to a fine dust particle size in order to enable this pneumatic transport on the one hand and to achieve short reaction times for the gasification of the individual particles on the other. In contrast to fluidised beds, no additional bed material is required here. [8, 9]

Since a dual fluidised bed gasifier is used in this plant, this, as well as fluidised bed gasifiers in general, will be discussed here more detailly.

2.1.2.1 Fluidised bed gasifiers

In this type of gasifier, a bed of fine bed material (usually quartz sand) rests on an inflow bottom. If the fluidisation agent passes through this bottom with a sufficiently high velocity (fluidisation velocity) the bed material is blown up and mixes with the fuel, a fluidised bed is created. The fuel particles are completely mixed with each other and the bed material. Thus, unlike with fixed bed gasifiers, no distinct temperature and reaction zones can form. Since the reactor has an almost constant, easily controllable temperature of about 700 - 900 °C, the individual partial reactions that take place during thermochemical conversion run in parallel. This smooth temperature distribution allows an easy controllability of the gasifier, which is the most important advantage of such systems. The intensive heat transfer from the bed material to the fuel particles as well as their large specific surface and the flow control reduce the residence time of the biogenic solid fuel in the reactor to a few seconds to minutes. [9]

Typically, fluidised bed gasifiers use air, water vapour or oxygen-vapour-mixtures as gasification agents. The gasification process can be carried out either under atmospheric pressure or under elevated pressure. The advantage of the higher pressure is on the one hand that the reactor dimensions can be reduced for the same

capacity and on the other hand that an already compressed gas is produced. However, due to the high plant engineering costs involved, this is primarily of interest for larger plant capacities. [9]

Due to their good heat transfer properties, fluidised bed gasifiers are ideally suited for allothermal gasification. Heat exchangers are arranged within the fluidised bed. Since the product gas leaves the reactor at high temperatures, heat exchangers are usually installed downstream for energy recovery. [9]

Compared to co-current gasifiers, the tar content is higher, but compared to counter-current gasifiers, it is significantly lower. However, the particle content in the product gas is drastically higher in fluidised bed gasifiers than in fixed bed gasifiers, as fine-grained material, ash or bed material is entrained with the product gas. [9]

In general, fluidised bed processes can be divided into three groups: [9]

- Stationary fluidised bed is characterised by the minimum fluidisation velocity, whereby, bed material and combustible are only put into a state of suspension.

- Circulating fluidised bed shows significantly higher gas velocity than necessary for fluidising the bed material. Therefore, a considerable amount of solid material is discharged with the gas and must then be separated by means of a cyclone and returned to the reactor.

- Dual fluidised bed is the combination of two fluidised beds to obtain a high-quality product gas. In this process, a fluidised bed is operated as steam gasifier (gasification zone) and the heat required for the gasification reactions is generated in a combustion fluidised bed (combustion zone) operated in parallel with air. The heat can then be transferred to the gasification zone by means of a circulating heat transfer medium or a high temperature heat exchanger (still under development).

The operating principle of a dual fluidised bed with circulating heat transfer medium is as follows: Biomass is introduced into the gasification zone and gasified there under the presence of steam. A medium calorific, practically nitrogen-free product gas is produced. In parallel, the necessary heat is produced in the combustion zone and this heat is transported to the gasification zone through the bed material circulating between the two fluidised beds. [9]

The temperature in the air fluidised combustion zone is usually 50 - 150 °C higher than in the gasification zone. The fuel required for the combustion can be introduced with the circulating bed material or, if necessary, externally into the combustion zone. The resulting exhaust gas is extracted separately from the product gas from the combustion zone. [9]

Such a system allows the production of high-quality product gas without the need for an air separation plant to produce pure oxygen. In addition, the combustion and gasification fluidised bed can be ideally designed independently of each other. Since

product gas and exhaust gas are not mixed but discharged separately, the measures for product gas cleaning are considerably less. [9]

A disadvantage is the increased complexity of such systems, which can only be justified if the benefits associated with the higher product gas quality are fully exploited.

Figure 4 shows the structure of such a dual fluidised bed. [9]

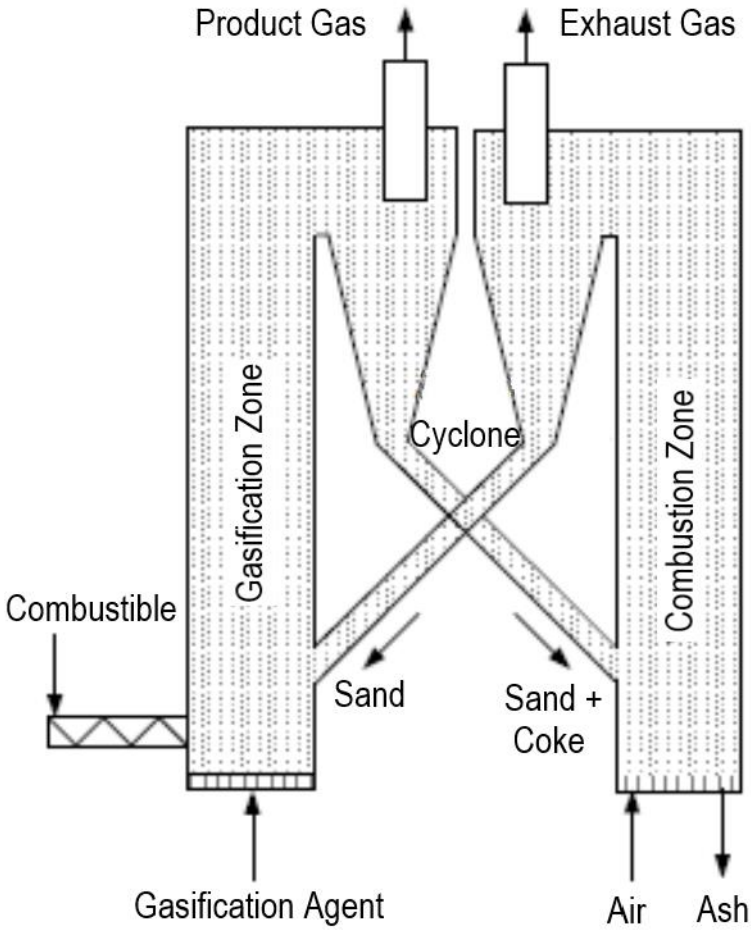

Figure 4: Schematic design of a dual fluidised bed (adapted from [9])

2.2 Synthesis gas

The term synthesis gas has been mentioned before. It describes gas mixtures which consist mainly of carbon monoxide (CO) and hydrogen (H_2) or of nitrogen (N_2) and hydrogen and can be used in synthesis reactions, for example to produce methanol (CH_3OH) or ammonia (NH_3). [10]

The original processes for synthesis gas production were initially based on the gasification of hard coal coke and brown coal semi-coke, with air and steam. In the middle of the last century liquid and gaseous raw materials (e.g.: crude oil and natural gas) were added as feedstocks. Their value lies in their higher hydrogen content. The H/C ratio for coal is 1:1, for crude oil already 2:1 and for methane-rich natural gas up to 4:1. [10]

Nowadays, biomass such as wood, peat or agricultural or urban waste is already being used for this purpose. In the latter case, however, pre-treatment of the materials used is usually still necessary. The production of synthesis gas by biomass gasification has already been discussed above, but the original processes and its use will be discussed here. [10]

2.2.1 Original production methods

2.2.1.1 Coal gasification

In coal gasification, coal is converted into a combustible mixture of carbon monoxide and hydrogen in a mixture of partial oxidation with air or pure oxygen and gasification with steam. The two most important reactions are the exothermic partial combustion of carbon (formula 2.8) and the endothermic heterogenous water gas shift (2.9). [10]

$$2C + O_2 \rightleftharpoons 2CO \qquad \Delta H = -221.6\ \mathrm{kJ/mol} \qquad (2.8)$$

$$C + H_2O \rightleftharpoons CO + H_2 \qquad \Delta H = 118.5\ \mathrm{kJ/mol} \qquad (2.9)$$

Of course, there are also other important reactions, which will not be discussed here in detail, but can be looked up in [10].

Characteristic for coal gasification processes are the high energy requirement to carry out the endothermic partial reactions and the high temperature level of at least 900 - 1000 °C to achieve the required reaction rate. The necessary heat input is either generated by reaction between the coal and the gasification agent, i.e. autothermal, or from another source, i.e. allothermal. [10]

The composition of the synthesis gas produced can be controlled by varying the feedstocks and process parameters. [10]

2.2.1.2 Oil and gas splitting

The production of synthesis gas from crude oil and natural gas is basically based on the same principle as coal gasification. This means a combination of exothermic and endothermic gasification reactions. There are two methods to convert crude oil fractions and natural gas:

1. Allothermal steam splitting

   The most common large-scale process used today is the so-called ICI process and consists of three stages. ICI stands for Industrial Chemical Industries and was a British chemical company that first carried out this process in 1962. [10]

   In the first stage the feed naphta (= crude gasoline; relatively light petroleum fraction obtained from crude oil by fractional distillation) is desulphurised. This is done by treating it with H_2 at 350 - 450 °C on a catalyst. The resulting H_2S (hydrogen sulphide) is adsorbed on ZnO (zinc oxide). At the same time any olefins present are hydrogenated. [10]

In the second stage, catalytic cracking in tubes (= tube cracking furnace, called primary reformer) takes place at about 800 °C and 15 - 40 bar. These tubes are heated by burning natural gas or ash-less distillates. With increasing pressure and constant temperature an increasing amount of methane remains. Since this is undesirable in synthesis gases, the product gas is passed through a Ni catalyst located in a shaft reactor (= secondary reformer). There a part of the gas is burned with the addition of air or oxygen and heated to over 1200 °C. During this process, the methane is converted with the steam to a residual content of about 0.25%vol. [10]

The advantage of this process is that no soot formation occurs, thus eliminating the need for catalyst regeneration. [10]

2. Autothermal cracking process

   Synthesis gas is produced by partial oxidation of petroleum fractions. All hydrocarbons from methane to heavy fuel oil are suitable for this. [10]

   The preheated feedstocks react with oxygen and water without a catalyst at approx. 30 - 80 bar and 1200 - 1500 °C in the combustion part of the reactor. With the help of the heat generated, the oil is split. Soot is produced from a small part of it. This is removed from the synthesis gas by washing with water or oil and pelletised. [10]

2.2.2 Cleaning

The synthesis gas resulting from the gasification of fossil fuels is contaminated with several gaseous compounds which are disturbing when used further. These include H_2S and COS (carbonyl sulphide), which are toxic to catalysts and can completely block their effectiveness, and CO_2 (carbon dioxide), which can lead to the formation of disturbing inert gas cushions. To eliminate these undesirable components, a variety of different gas scrubbing processes are available. For example, the Rectisol process, which is based on pressure washing with methanol; the Selexol process, which exploits the pressure-dependent solubility of acid gases in dimethyl ethers of polyglycols; or the Sulfinol process, which uses sulpholane/diisopropanolamine mixtures. Some methods of gas cleaning relevant for this work are discussed in the chapter after the problematic substances (tars). [10, 11]

2.2.3 Usage

On the one hand, synthesis gas can be used directly to generate energy in power plants, for example as fuel gas in combustion engines or in special hydrogen gas turbines, and thus be converted into electricity and heat. On the other hand, it can be used as a starting material for various conversion processes for chemicals and fuel production. In this context, the methanol-, oxo-, and Fischer-Tropsch-synthesis should be mentioned in particular. Figure 5 schematically illustrates the different possible uses. [12]

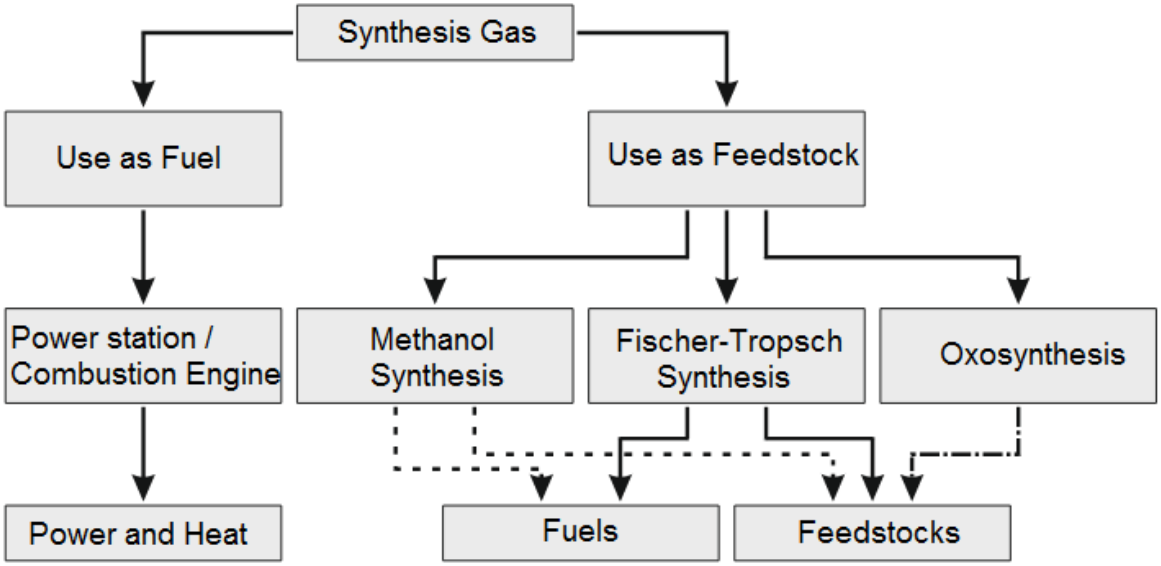

Figure 5: Process scheme for the direct use of synthesis gas (adapted from [12])

2.3 Tars

Tars, such as those produced during biomass gasification (pyrolysis), are complex mixtures of hydrocarbon compounds. There is no uniform definition for them. In general, however, all organic components with a molecular weight greater than benzene (78 g/mol) are understood as tars. [9]

What proves to be problematic is their behaviour of forming deposits during condensation, as soon as the gas flows through cool plant components and is compressed. This can lead to sticking or clogging and therefore, must be prevented. However, even deliberately deposited tars still prove to be a problem, as they are acutely toxic and therefore, represent both a health and environmental problem. Therefore, tar should not only be removed from the raw gas, but its formation should already be reduced by choosing suitable gasification processes. [9, 13]

2.3.1 Origin

As mentioned above, the properties of tar depend on different parameters. Firstly, the material used, its elementary composition and its structure. Also, the process parameters and the process itself play a major role for the formation of tars. In particular, the heating rate and the maximum temperature reached have a great influence. In addition, the gas phase composition, its temperature and above all the presence of oxygen as influencing factors.

2.3.1.1 Pyrolysis

Pyrolysis is the thermal decomposition of organic matter under lack or absence of oxygen. During this process step, which takes place at about 200 – 700 °C, the volatile components of the fuel are released. In addition to volatile hydrocarbons and steam, these include the combustible gas components CO, H_2 and CH_4. In the case of biomass, up to 85% of the fuel mass is transferred to the gas or liquid phase in this way. [13, 14]

If the pyrolysis takes place under mild conditions, substances with oxygen-containing functional groups are formed. However, if the whole process takes place at higher temperatures and heating rates, the functional groups are released as CO, CO_2 and H_2O and the remaining components are stable, mainly aromatic compounds. [14]

Figure 6 shows the mechanisms of pyrolysis and the resulting substances.

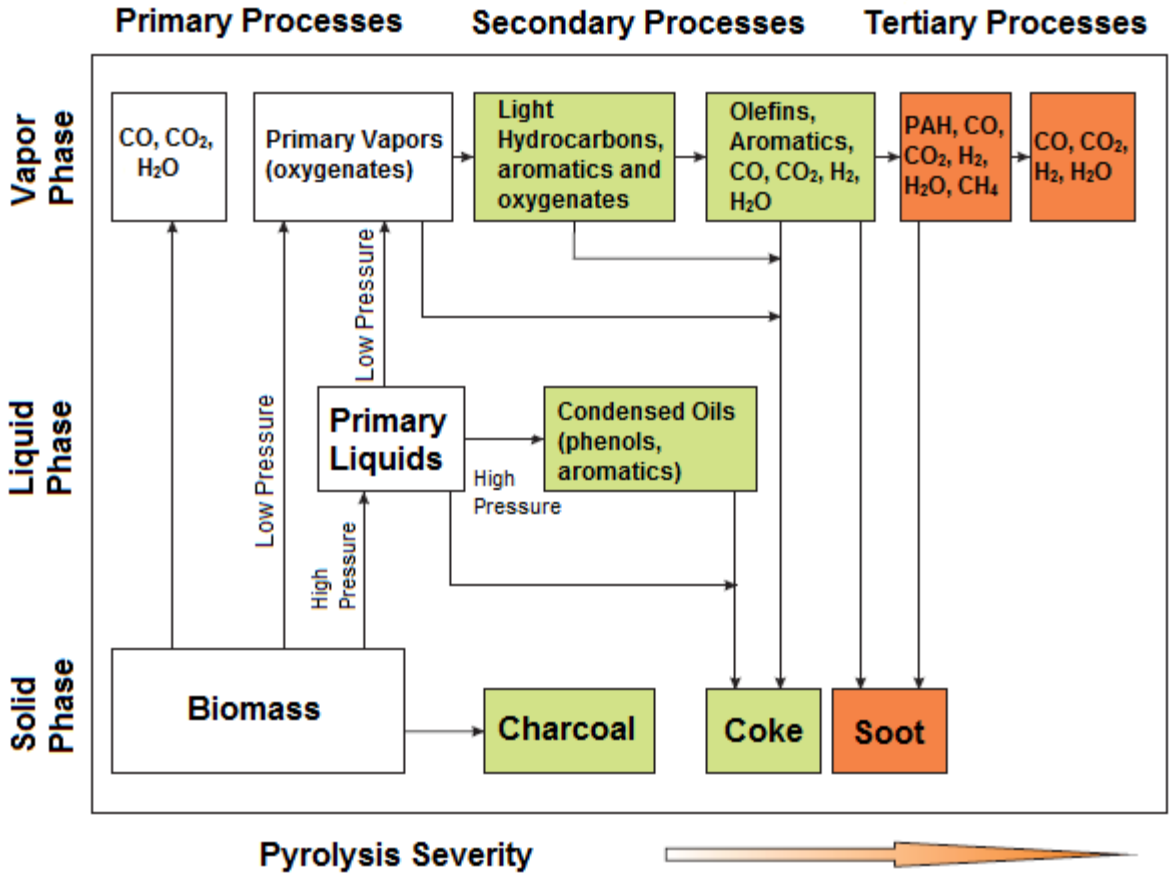

Figure 6: Pyrolysis mechanisms of biomass (adapted from [14])

2.3.1.2 Polycyclic aromatic hydrocarbons (PAH)

When the products of the pyrolysis zones pass through high temperature zones (from approx. 800 °C), tar is formed which mainly consists of polycyclic aromatic hydrocarbons (PAH). The benzene ring forms the basic structure of this substance class. The simplest PAH is naphthalene, which consists of two conjugated benzene rings. PAH are very stable compounds. Many of them are proven to be carcinogenic,

so they should be handled with care. The tars that form in the gas of circulating and stationary fluidised bed gasifiers as well as co-current fixed bed gasifiers consist mainly of aromatic compounds and PAH. [13, 14]

2.3.2 Tar classification

As tars differ depending on the fuel, the type of conversion process and the conditions prevailing, there are also different ways of classifying them: [13]

- By origin (low/high temperature or primary, secondary and tertiary tars)
- By the process (pyrolysis tar, smouldering tar, gasification tar)
- After the analysis or the properties [e.g: Total tar, gravimetric tars, GC detectable tars, five class system according to ECN (Energy Research Centre of the Netherlands)].

If the tars are not to be separated but transformed in the process, the components can also be divided into those that are easy to destroy and those that are difficult to destroy. [13]

Looking at the origins, the most frequently cited model is probably that of Milne and Evans (1998). They divide the constituents of tar into primary, secondary and tertiary tar components according to their formation within temperature-dependent process stages. Shown in Figure 7. [13, 15]

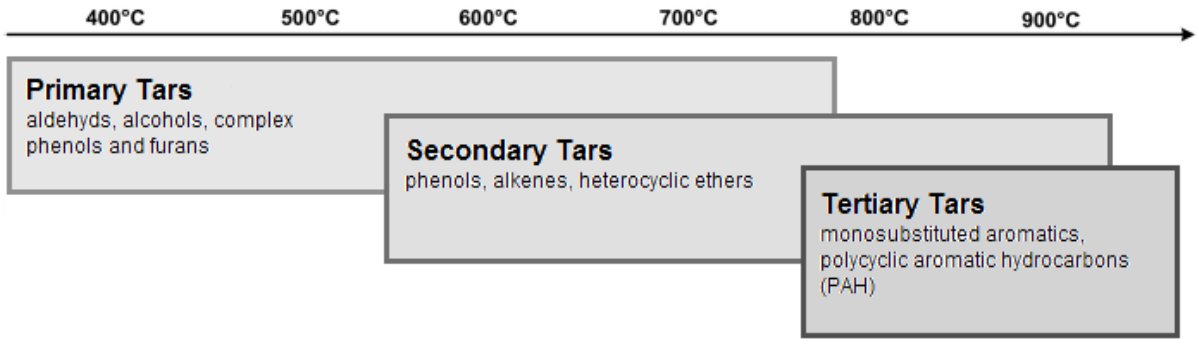

Figure 7: Classification of tars according to their origin (adapted from [13])

The ECN divides tars into five classes according to their physical properties in terms of water solubility and condensation behaviour. This classification is shown in Table 2.

Table 2: Tar classes according to ECN (adapted from [14])

Tar Class	Designation	Properties	Typical Components
1	not GC detectable	Very heavy tars that are not detectable with GC	furfural, hydroxyacetaldehyde
2	heterocyclic compounds	Tars with heteroatoms; highly water-soluble compounds	pyridine, phenol, benzonitrile, quinoline, dibenzophenol
3	light aromatics	Light hydrocarbons, which have no relevance for problems with condensation and water solubility	xylene, styrene, toluene
4	light polyaromatics	Condensate only in high concentration at medium temperatures	naphthalene, biphenyl, fluorene, anthracene
5	heavy polyaromatics	Condensate even in low concentrations at high temperatures	fluoranthene, pyrene, chrysene, benzofluoranthene, perylene

2.3.3 Components of raw gas

This subchapter gives a short overview of the properties of some components found in raw gas and also used in these experiments. In addition, applications of these substances in the chemical industry are shown.

2.3.3.1 BTX

The aromatic hydrocarbons benzene, toluene and xylene are often abbreviated as BTX. These are flammable, colourless liquids with a characteristic (aromatic) odour. They are miscible with organic solvents. In the past, these aromatics were mainly obtained by distillation from hard coal and by leaching from coke oven gas. Their increasing demand led to the development of petroleum-based production processes. In the petroleum refining process, for example, aromatic-rich fractions occur simultaneously in the gasoline refining by reforming and in the cracking processes for olefin production. As reformate gasoline and cracked gasoline, they are important sources for the production of BTX aromatics. [16]

Benzene (C_6H_6) is an important base/bulk material in the chemical industry, especially for the production of plastics (polystyrene, polyamides), synthetic rubber, dyes, insecticides, etc. However, it is no longer used as a solvent due to its carcinogenic effect. The annual global production is over 35 million tons per year. Figure 8 shows the classic symbolisation of the benzene ring. [17, 18, 19]

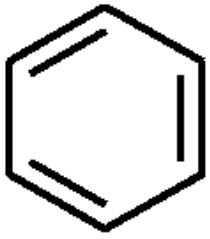

Figure 8: Structural formula of benzene [18]

Toluene (C_7H_8) is used particularly as a solvent for paints, resins, varnishes and plastics and as an admixture in engine fuels. It is harmful to health and, in high concentrations, can lead to liver and heart dysfunction and to changes in the blood count. [17, 18]

Xylenes (C_8H_{10}) are aromatic compounds that have two methyl groups in addition to the benzene ring. There are three different positional isomers, ortho-, meta- and para-xylene. Technical xylene is a mixture of the three isomers and usually contains up to 20% ethylbenzene. Xylenes are used as solvents for fats, oils, resins, lacquers and paints as well as for metal degreasing. O-and p-xylene are also used as starting products for the production of phthalic anhydride and terephthalic acid. [16, 17, 18, 19]

2.3.3.2 Thiophene

Thiophene (C_4H_4S) is a component of coal tar and is often extracted together with benzene. Due to its aromatic character, it shows great chemical and physical similarities with benzene. This makes it difficult to separate the two substances. It is immiscible with water, but is easily soluble in ethanol, ether, trichloromethane and benzene. The vapours of thiophene cause severe irritation and damage to the eyes, respiratory tract, lungs and skin. It is particularly used in the production of pesticides, dyes and aromas. Its derivatives are important as active pharmaceutical ingredients and serve as pharmaceuticals. [18]

2.3.3.3 Styrene

Styrene (C_8H_8) is found in coal and lignite tar. It is most commonly produced by direct catalytic dehydrogenation of ethylbenzene. It is only very slightly soluble in water, but good in ethanol, methanol and acetone. The vapours of this substance may cause irritation of the eyes, skin and upper respiratory tract. Besides ethene and vinyl chloride, styrene is the most important monomer for the production of thermoplastics. When processed into polystyrene, it is used especially for packaging, electrical appliances, toys and insulating materials. [18]

2.3.3.4 Naphthalene

Naphthalene ($C_{10}H_8$) is produced during the dry distillation of hard coal. Technical naphthalene is obtained from refinery products, from the medium and heavy oils of coal tar and by catalytic hydrodesalkylation. It is insoluble in water, but easily soluble in alcohol, ether, trichloromethane and benzene. Inhalation of this substance can lead to cataracts, eczema and blood damage. Naphthalene and its derivatives are starting materials for tanning and dyeing agents, insecticides and pharmaceuticals. [18]

2.3.4 Market prices

Due to their hazardous properties, but also due to their economic importance in relation to the various industrial sectors, the separation of all these previously treated substances is of great value.

The following sub-chapter is intended to give a brief overview of the current market prices of some of these substances in Europe. Unfortunately, these prices are difficult to determine without access to a portal for raw material prices, so the prices given here should be treated with caution.

In the last decade, benzene consumption has shifted from Europe and North America to Asia (Middle East, North, South East Asia). China in particular has become an increasingly important influencing factor on the benzene market. China's consumption has increased by an average of 9% per year since 2013. With the exception of North America and the Middle East, consumption in all other regions has declined over the same period. Figure 9 shows the global consumption of benzene. [20]

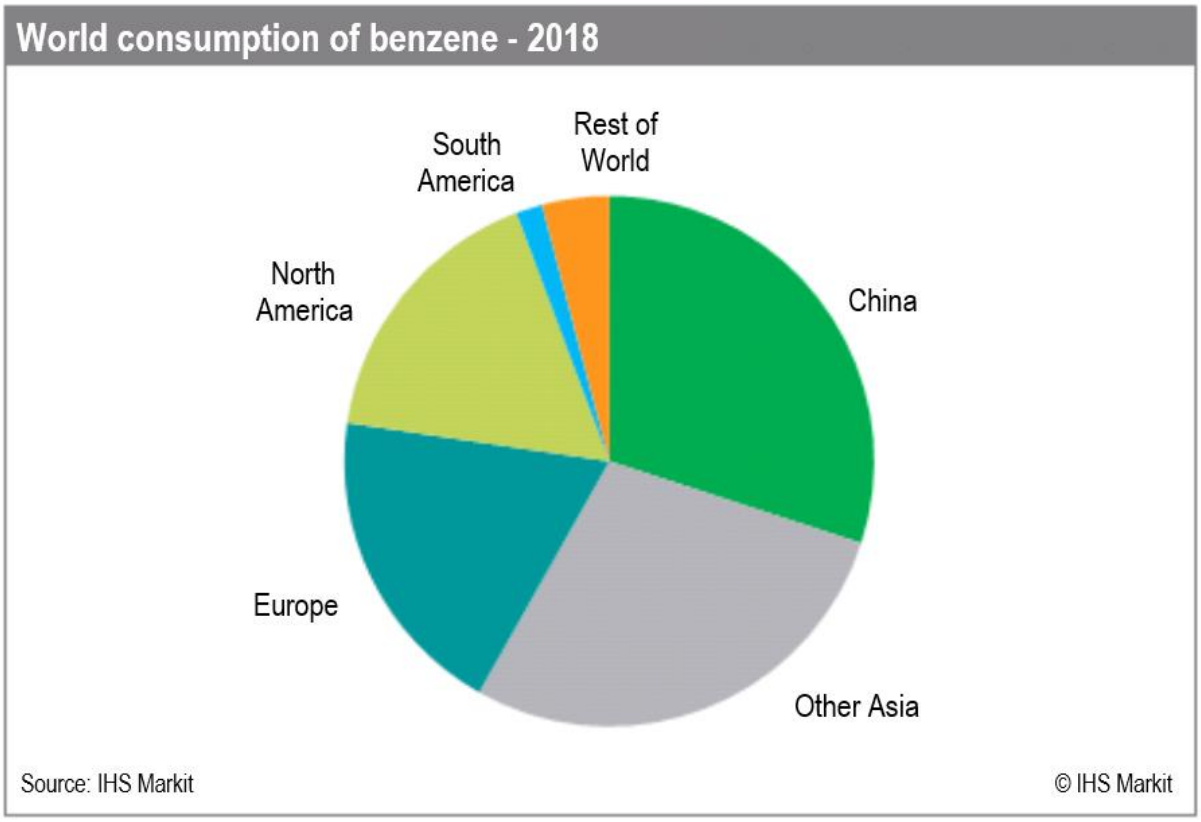

Figure 9: Global distribution of benzene consumption [20]

In 2016, the world market for benzene was 45 million tonnes, with an annual growth rate of 3%, this means that in 2019 it was around 50 million tonnes. In 2019, the price of benzene in Europe averaged 630 €/t. Over the course of the year, it can be seen that the price was lowest in the winter months and reached its high in summer, especially August and September, at around 730 €/t. Compared to 2018, however, the price has fallen sharply. At that time. The average price was around 720 €/t. Furthermore, the price in 2019 was subject to strong fluctuations in some cases, from just under 500 to 730 €/t. In the previous year it was almost constant between 700 and

770 €/t. At the end of 2019, the price was around 570 €/t. An increase in the price is expected at the beginning of 2020, as there will be announced maintenance work on some plants in Asia, among other places, and thus a reduction in production capacity. Overall, benzene consumption is largely linked to the general economy and is increasingly associated with emerging markets (especially China). This is due to the improvement in living standards, which leads to an increasing use of a wide range of chemicals and polymers. Thus, steady growth can be expected in the coming years. [20, 21, 22]

The same applies to toluene as to benzene. Consumption in the western industrialised countries is declining slightly, but due to the increase in Asia, especially China again, total capacity will increase in the coming years. Currently about 24 million tons are produced annually. In 2019, the average price was around 715 €/t, although here too it peaked during the summer months. At the end of the year it was around 660 €/t. A slight increase is also expected here. Furthermore, the consumption of toluene will increase steadily in the coming years. [20, 21, 23]

Mixed xylene is the second most important aromatic product after benzene, and even before toluene, in terms of global consumption for the chemical industry. In 2016, world production was around 50 million tonnes, with a projected growth rate of around 4% per year. This would mean that in 2019 about 56 million tonnes would be produced. Typically, xylene consists of 40-65% of m-xylene (MX) and up to 20% each of o-xylene (OX), p-xylene (PX) and ethylbenzene. In recent years, large investments have been made in mixed xylene capacity, especially for p-xylene. Due to its large population and the increasing demand for polyester fibers and resins and the corresponding growth in this industry, the largest market is again the Asian one, with South Korea being particularly strong in this case, in addition to China. PX is the most widespread and is primarily used to obtain terephthalic acid (PTA), which is also needed for polyethylene terephthalate (PET) for the production of polyester fibers. OX is especially isolated to produce phthalic anhydride, which is used as a plasticiser in the production of PVC products. MX is used for the production of isophthalic acid and subsequently for plastic bottles. The price for PX is currently around 770 €/t but was already 1,000 €/t in April 2019. The price for OX is about 820 €/t, whereas in May of last year it was 960 €/t and for the whole year 2019 it was about 865 €/t. Prices for MX and mixed xylene could unfortunately not be determined. Over the next five years, capacity for blended xylene is expected to increase by an average of 4-5% per year, mainly due to new investments in China, Southeast Asia and the Middle East, while consumption is expected to increase by an average of 3-4% per year. [20, 21, 23, 25, 26]

Figure 10 shows possible production increases of various chemicals, including BTX, for 2030 and 2050, modelled with two different scenarios: RTS, the Reference Technology Scenario, and CTS, the Clean Technology Scenario. The former is based on a correlation between current energy prices and the demand for chemicals, based on existing and announced policies. In contrast, the CTS works from a predefined point in the future, derived from the United Nations goals of sustainable development, back to the present. Among other things, it is assumed that there will be more recycling than at present, which in turn will lead to less "new production" of various chemicals. [27]

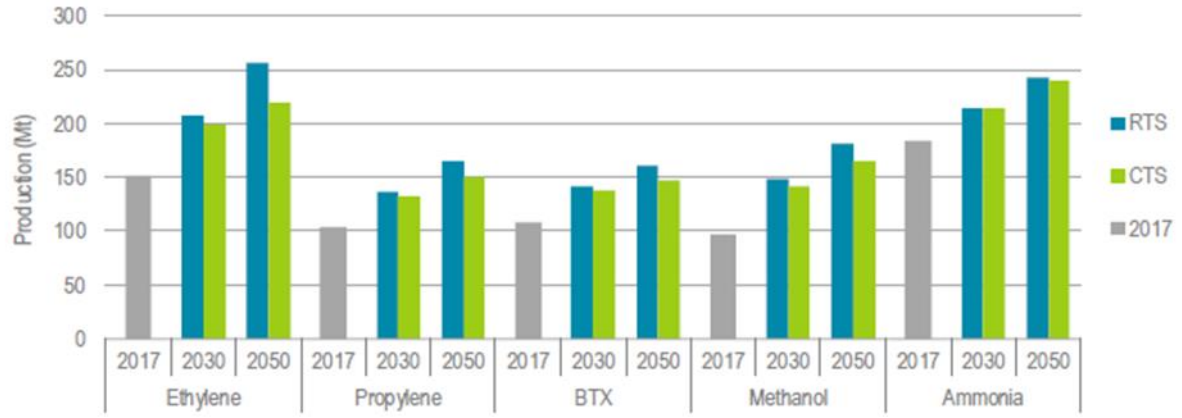

Note: Mt = million tonnes.

Figure 10: Global production of various chemicals by scenario [27]

Update due to the COVID-19 crisis: After the predicted increase in the price of benzene at the beginning of 2020, the COVID-19 pandemic in March led to significant declines in economic output in all industrialised countries and most recently also in emerging and developing countries. In China, gross domestic product (GDP) fell by 6.8% compared with the previous year due to the lockdown measures in the first quarter. In the EU, GDP was around 3.5% lower. Prices for various chemicals developed accordingly. The price of benzene, for example, fell by 70% in April compared to the first quarter, that of OX by 35% and that of PX by 30%, see Fig. 11. As a result, it is not possible to make any precise statements regarding future production and price developments. [28]

IMPORTANT PRICES FOR THE CHEMICAL INDUSTRY

Naphtha and contract prices in euro, change in percent

Product	2019 Q3	2019 Q4	2020 Q1	2020 April-May
Naphtha	432	465	381	140*
compared to previous quarter	– 11.3	+ 7.7	– 18.0	– 63.3
Ethylene	993	973	953	670
compared to previous quarter	– 6.7	– 2.0	– 2.1	– 29.7
Propylene	893	852	838	610
compared to previous quarter	– 9.2	– 4.7	– 1.6	– 27.2
Benzene	692	618	672	199
compared to previous quarter	+ 8.0	– 10.6	+ 8.7	– 70.5
o-Xylene	845	817	800	520*
compared to previous quarter	– 10.3	– 3.4	– 2.0	– 35.0
p-Xylene	774	763	704	493*
compared to previous quarter	– 14.5	– 1.3	– 7.7	– 30.1

Sources: ICIS, eid, VCI * April 2020

Figure 11: Price changes in recent months; immense drop due to COVID-19 (adapted from [28])

Styrene is one of the most important products of the petrochemical industry. Its market value in 2012 was approximately € 38 billion. About 40% of styrene is used to produce polystyrene, which is used as a packaging material mainly in the food and electrical industries. It is also true for styrene that consumption in the USA, Europe and South America has fallen slightly in recent years. The Northeast Asian market (China, Japan, Taiwan and South Korea), led by China, remains the dominant player in the styrene industry. Overall annual growth of 2% is expected in the coming years. In 2018, the price fluctuated very strongly. In the first quarter, it was as high as 1,450 €/t, but fell to just under 1,000 €/t by the end of the year. In 2019, it rose to around 1,200 €/t by the middle of the year but ended the year below 1,000 €/t again. It is still in this range at the moment. [20, 24, 25]

Unfortunately, no results were found for thiophene.

It was difficult to find market prices for naphthalene in Europe. On the Chinese market, it fluctuated between 610 €/t at the beginning of 2019 and 400 €/t in October. The year ended with a price of 510 €/t. In the Western countries and Japan, growth of less than 1% is expected in the next few years, while in the developing regions (India, the Middle East and above all China again) growth of 3-4% is forecast. [22]

In general, it can be said that the demand for the substances discussed will increase throughout the next few years. However, this is particularly due to the Asian market, above all China, and does not necessarily apply to Europe as well. In part, the market prices are strongly related to the price of crude oil, as they are largely derived from it. In turn, some price fluctuations can be explained by, in part unexpected, maintenance work on large plants.

The research on market prices and forecasts for the coming years was carried out before the worldwide COVID-19 crisis and should therefore be treated with even greater caution.

2.4 Methods of gas cleaning

Due to the high purity requirements for synthesis gas, gas purification is extremely important in biomass gasification. Nitrogen-based impurities (e.g. ammonia, hydrocyanic acid), halogen-based impurities (e.g. hydrochloric acid), sulphur-based impurities (e.g. hydrogen sulphide) and higher hydrocarbons (tar) have a negative impact on the service life of the process steps required for synthesis, especially the catalytic processes. They must therefore be removed before use in synthesis gas processes. Table 3 shows typical impurities in product gas from biomass gasification. Besides these, there are of course other impurities, but as they are not part of this work, they will not be discussed further. [6, 29]

Table 3: Typical impurities in raw gas from biomass gasification (adapted from [29])

Particles	g/m^3_{STP}	10-100
Tars (incl. BTX)	g/m^3_{STP}	2-20
Ammonia	ppm	200-2,000
HCN (=hydrocyanic acid)	ppm	10-100
H_2S (=hydrogen sulphide)	ppm	50-100
COS (=carbonyl sulfide)	ppm	2-10
Halogens	ppm	0-300
Alkali metals	ppm	0.5-5

If DFB gasifiers are operated at higher temperatures, this leads to a reduction of the total tar quantity. At the same time, however, this promotes the formation of higher aromatics and polyaromatic hydrocarbons (PAH) by reducing the oxygen in the structures. [6]

There are different methods to obtain low-emission gas. Primary measures aim to take care already during the design and construction of such a plant that in the end, less impurities are produced. Removal of undesirable components afterwards is categorised as secondary measures. This refers to a wide variety of physical and chemical processes for gas cleaning. They can be roughly divided into cold gas and hot gas cleaning processes. [6, 30, 31]

2.4.1 Cold gas cleaning

A distinction is made between dry and wet processes. Dry processes include filtering separators (packed bed and bag filters) and centrifugal separators (cyclones). Although these separate particles and alkalis sufficiently, other pollutants are only removed to a limited extent. Wet processes (scrubbers, wet electro-filters), on the other hand, enable not only the separation of particles but also of tars and other undesirable components. [30]

2.4.2 Hot gas cleaning

These processes are primarily used to recycle the gas in a gas turbine or fuel cell, as the gas can be fed directly into the turbine combustion chamber without first having to be cooled down. Catalysts can be used to reduce tars. However, these are susceptible to other pollutants such as chlorine and sulphur. Filtering or centrifugal separators, on the other hand, make it possible to remove particles and alkalis. [30]

2.4.3 Physical methods

The following section gives a brief overview of the physical processes of gas cleaning. Most of them, such as filters and scrubbers, operate at low and medium temperatures. Cyclones, however, can also be used for hot gas.

Cyclones: Cyclones can be used to separate high particle loads from a gas stream. Therefore, they are mostly used for initial cleaning. Particles are solids that are discharged from the gasifier with the raw product gas. These include unreacted biomass, bed material or inorganic ash. In addition to the effectiveness of cyclones, their relatively inexpensive construction and operation are also advantageous. They are particularly effective with large particles and can be used over a wide temperature range. Their separation efficiency decreases drastically for small (<5µm) particles. Especially carbonaceous particles, which are often produced during gasification, are removed from them only very poorly, due to their small particle size. [30]

Filters: Filters can separate particles in the range of 0.5 - 100µm very effectively. They can remove even smaller particles. However, since this would involve an enormous pressure loss, such filters are only used for particles larger than 0.5µm for technical and economic reasons. Due to the formation of a filter cake, filters must be cleaned from time to time by means of pressure pulses acting against the actual direction of inflow. In order to keep cleaning intervals low and thus save operating costs, filters are usually used in combination with cyclones, which have already removed the coarse particles before. [30]

Standard fabric filters can be used up to a temperature of approx. 250 °C, metal fabric filters up to approx. 350 °C. If there are tars in the product gas, this can cause the filter to stick. Therefore, they must be separated beforehand or the condensation temperature of the tars must not be allowed to fall below. Precoating offers a possibility to remove both dust and tars at the same time and to prevent sticking. This means that the filter medium is coated with an auxiliary agent which takes over the filter effect and is then removed together with the separated mixture of dust and tar. With this method, dust can be filtered out to a very high degree and also up to 80% of the tar can be removed. [9, 30]

A further possibility to separate dust and tar simultaneously is the use of *packed bed filters*. Here the gas flows through a bed, which can consist of various materials, such as sand, ceramic balls or sawdust. They are mainly used for small plants. Their big

disadvantage is that the filter material loaded with toxic tar cannot be regenerated and therefore has to be disposed of at high costs. [9, 30]

Cartridge filters, also known as hot gas filters, can be used at temperatures up to 900 °C. They are made of metal or ceramic and have the advantage that the gas does not have to be cooled beforehand. Their disadvantage, in turn, is that they can clog or stick. [9, 30]

Electrical separators: These use the force effect on charged particles in the electrical field to separate dust. They can be operated at up to 500 °C and are usually used for cleaning large quantities of gas. In the simplest case, they consist of a grounded tube with a spray electrode in the middle. This releases electrical charges which charge the dust particles. These are then attracted by the pipe, the so-called precipitation electrode, where they adhere and form a layer of dust. The removal of this layer and the transport into a dust collection container can be done in a dry or wet way. So, either by tapping on the collecting electrode, whereby the particles fall into a container, or they are transported there by a sprayed or condensed liquid film. Advantages of this type of filter are the low pressure loss and the low operating costs. Disadvantages are the large space requirement and the initially high investment costs. [30, 32]

Scrubbers: Here a scrubbing liquid (e.g. water) is used to remove particles from the gas. Typical designs are washing towers, jet, vortex, rotary and Venturi scrubbers. Depending on their design, the various scrubbers differ in their separation efficiency for pollutants and pressure loss. What they all have in common is that the inlet temperature of the raw gas must be below the evaporation temperatures of the scrubbing liquid (e.g. 100 °C for water). Therefore, the gas must first be cooled. Due to the gas scrubbing process, dirty washing agent is produced which has to be treated for regeneration or disposal. Thus, scrubbers have relatively low investment costs, but their operating costs are high. Figure 12 shows the most common wet scrubbers and their main characteristics. [9, 30]

	Washing Tower	Jet Scrubber	Vortex Scrubber	Rotary Scrubber	Venturi Scrubber
	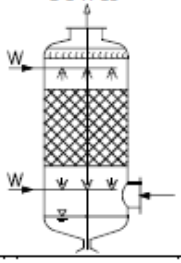	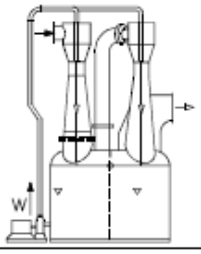	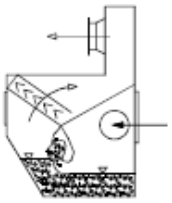	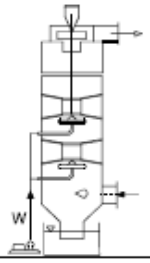	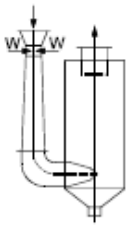
Separation grain size in µm for ρ=2.42 g/cm³	0.7 – 1.5	0.8 – 0.9	0.6 – 0.9	0.1 – 0.5	0.05 – 0.2
Relative speed in m/s	1	10 – 25	8 – 20	25 – 70	40 – 150
pressure loss in mbar	2 – 25	–	15 – 28	4 – 10	30 – 200
Water/gas in l/m³	0.05 – 5	5 – 20[a]	undefined	1 – 3[a]	0.5 – 5
Energy consumption in kWh/1000m³	0.2 – 1.5	1.2 – 3	1 – 2	2 – 6	1.5 – 6

[a] per stage; ρ density

Figure 12: Wet scrubbers and their most important parameters (adapted from [9])

In the past, water was often used as a detergent. Since tar is only poorly soluble in it, however, the separation efficiency is very weak. Problems such as clogging, foaming and tar-contaminated wastewater often occur. [7]

If, on the other hand, oily detergent is used to separate tar, the separation efficiency increases because tar is absorbed from the gas. Tar contents of 10 mg/m³$_{STP}$ can be achieved. The loaded detergent can be incinerated or cleaned with a stripper. Biodiesel is often used as a detergent. In Europe, RME (rapeseed methyl ester) is suitable due to its regional availability. This has proven to be the most suitable before rapeseed oil and fuel oil EL (extra light) and is characterised by low viscosity, low vapour pressure and strong solubility of naphthalene (as a model for tar). [7, 9, 30]

The reason for the experiments in this work was to find out whether a TSA could replace an RME-scrubber, so this will be briefly discussed here.

RME-scrubber: In this scrubber the cooled RME passes through a liquid distributor onto a structured packing. As it flows down, it wets the packing and absorbs tar from the product gas flowing in counter-current. It also cools the gas below the dew point, causing water to condense. [7]

Below the scrubber is a basin in which the condensate and RME are separated. This is due to the difference in density between the two liquids. The oily RME floats on the aqueous condensate. The emulsion, which flows continuously from above, leads the RME via an overflow into a second tank. Here fresh RME is additionally fed in, returned to the liquid distributor, and cooled on the way there. [7]

Usually two more liquid streams are led out of the first tank. The first, at about half height of the tank, is a small amount of condensate-RME-emulsion. This part contains

loaded RME and is burned in a combustion chamber. This prevents the accumulation of tar and dust particles in the boundary layer. Second is the condensate. Volatile components are first expelled from the condensate in a condensate evaporator and also burned. Afterwards, steam for gasification is produced in the steam generator by adding heat. [7]

Due to the experiments which were made for this work and which dealt with the temperature swing adsorption, the adsorption is described here in more detail.

2.5 Adsorption

Adsorption is the binding of molecules from a gas or liquid phase to the surface of a solid. This is an exothermic process, i.e. adsorption heat is released. Desorption is the reversal process of this, namely the release of bound molecules to the fluid phase and takes place endothermically. [33]

Particles which are in the fluid phase as well as particles which are already bound by a solid, the adsorbent, are called adsorbate. All these terms are shown graphically in Figure 13. [34]

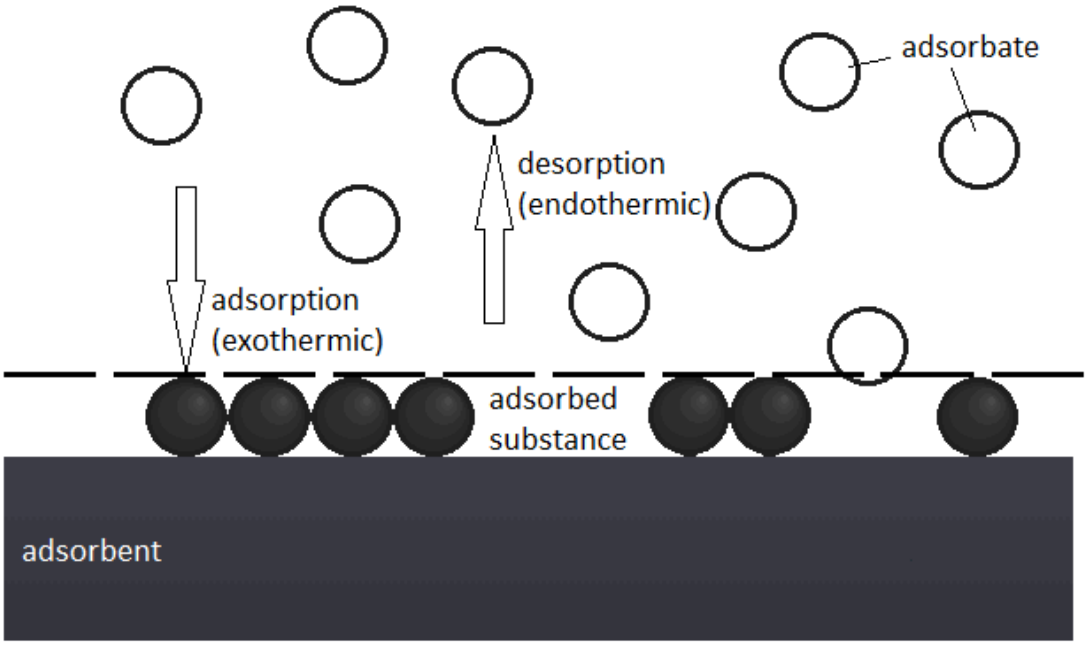

Figure 13: Graphical representation of the basic concepts of adsorption

Depending on the type of bond, a distinction is made between physical and chemical adsorption. In physisorption, electrostatic forces of attraction, the so-called van der Waals forces, act. Due to the short range of these forces, there is only a loose bond between adsorbent and adsorbate, which can easily be dissolved again. [35]

In chemisorption, the bond between adsorbent and adsorbate is created by valence forces. This means that there is a chemical bond which is difficult, if at all, to dissolve again. [35]

In process engineering, adsorption is a widely used process due to its high separation efficiency and selectivity. The possible applications range from the purification of waste gases from waste incineration plants to the treatment of drinking water and the extraction of oxygen, nitrogen and noble gases from air. [34]

In exhaust gas cleaning, the removal of pollutants is usually done by the gas stream passing through a fixed adsorbent bed and pass the adsorbate from the gaseous phase to the solid. Once the fixed bed is loaded, it must be regenerated. This offers the opportunity to recover the pollutants and to use them for further applications. [36]

2.5.1 Basics of adsorption

As with all thermal separation processes, the driving force for adsorption is an imbalance imposed from the outside. Based on this imbalance, the system tries to achieve a new state of equilibrium during the process. The position of this state of equilibrium is described by thermodynamics, the velocity at which the new equilibrium is sought is determined by kinetics. The processes involved in gas phase processes are described below. [34]

2.5.2 Thermodynamics of adsorption

The adsorption equilibrium describes the relationship between the concentration of a pollutant component in the gas and the loading of this component on the adsorbent. In principle, the thermodynamic equilibrium can be described in three ways, shown in Fig. 14.: [34, 36]

1. Via adsorption isotherms (common representation): that means the ratio between the adsorbed volume (= loading X of the adsorbent) and the partial pressure (P_A) of the adsorbate at constant temperature (T) (see Fig. 14.a)

2. Via adsorption isosteres: that means the ratio between (partial) pressure and temperature at a constant adsorbed volume (see Fig. 14.b)

3. Via adsorption isobars: that means the ratio between the adsorbed volume and the temperature at constant pressure (see Fig. 14.c) [34]

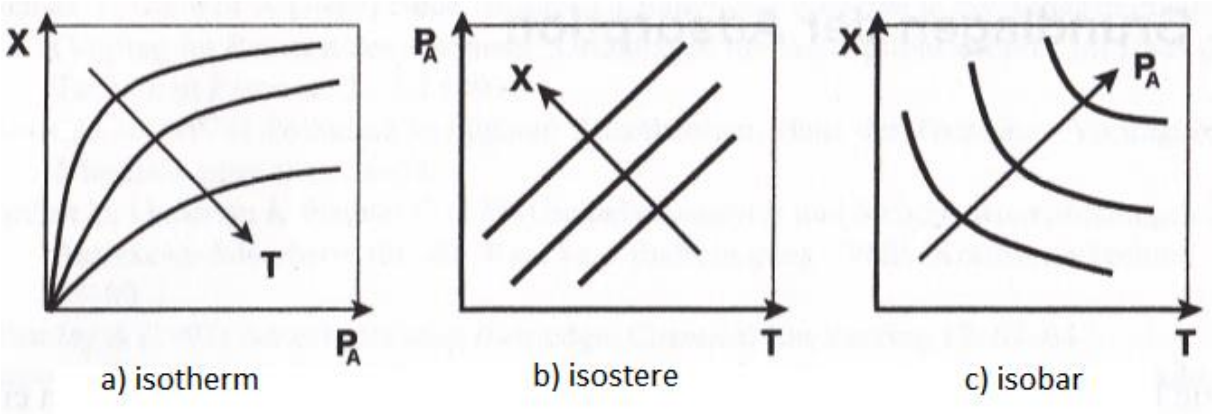

Figure 14: Representation of the thermodynamic equilibrium during adsorption (adapted from [34])

The simplest case of adsorption is one-component processes, which occur only rarely in industrial practice. Usually these are multi-component processes. However, since it can often be assumed that certain components behave inertly, i.e. are not adsorbed, or one substance is dominant, these processes can be described using single-component isotherms. Several equations are available for this purpose, the most common ones being described below. [33, 34]

2.5.2.1 Henry equation

The simplest isothermal equation is the linear Henry equation. It assumes that there are no interactions between the adsorbed molecules and that all adsorption sites are energetically equivalent and can be occupied. [34]

$$X = k_H * p_A \qquad (2.10)$$

X represents the actual loading of the adsorbent, k_H is the Henry constant and p_A is the partial pressure of the adsorbate in the fluid phase.

This equation is not thermodynamically derivable and thus, should be considered with caution in the scientific sense. Its use only makes sense for areas of low concentration or loading. [34]

2.5.2.2 Langmuir equation

This two-parameter equation can be derived thermodynamically and requires the following assumptions: a monomolecular coverage of the adsorbent surface, a constant adsorption enthalpy and all adsorption centers are equivalent and cover the surface uniformly. [33, 34]

$$\frac{X}{X_m} = \frac{b * p_A}{1 + b * p_A} \qquad (2.11)$$

X_m is the maximum possible monomolecular load and b is a constant. [33, 34]

2.5.2.3 Freundlich equation

This isotherm equation takes interactions between the adsorbed particles into account. This means that the more molecules are already bound to the adsorbent, the more difficult it is to adsorb further molecules. Graphically this means a flattening of the curve. [34]

$$\mathrm{X} = k * {p_A}^n \qquad (2.12)$$

Each k and n are constants of the Freundlich equation. [34]

2.5.2.4 Equation according to Brunauer, Emmet and Teller (BET)

This equation is based on the Langmuir equation and allows the description of multi-layer adsorption. It is assumed that in the first bound layer the constant adsorption energy, which is composed of evaporation and binding energy, is released, but for each additional layer only the evaporation energy. [33, 34, 37]

$$\frac{X}{X_m} = \frac{\frac{p_A}{p_{tot}}}{1 - \frac{p_A}{p_{tot}}} * \frac{b}{1 + (b-1) * \frac{p_A}{p_{tot}}} \qquad (2.13)$$

P_{tot} stands for the total pressure of the system. If there is only one monomolecular bond, then the BET equation changes to the Langmuir equation. [33, 34, 37]

2.5.3 Kinetics of adsorption

The kinetics describes the dependence between the speed at which the approximation process during adsorption takes place and the various influencing variables. This process takes place in the following sub-steps, which are also illustrated in Fig. 15: [34, 37]

1. Mass transfer (diffusion) through the laminar boundary layer surrounding the particle

2. Mass transport through the pores filled with fluid inside the particles and on the adsorbent surface

3. Condensation of the molecules on the inner surface (= adsorption)

Adsorption (3) releases the adsorption enthalpy. The resulting heat is dissipated to the environment by the adsorbent and the outer boundary layer.

4. Energy transport in the adsorbent

5. Energy transport through the boundary layer

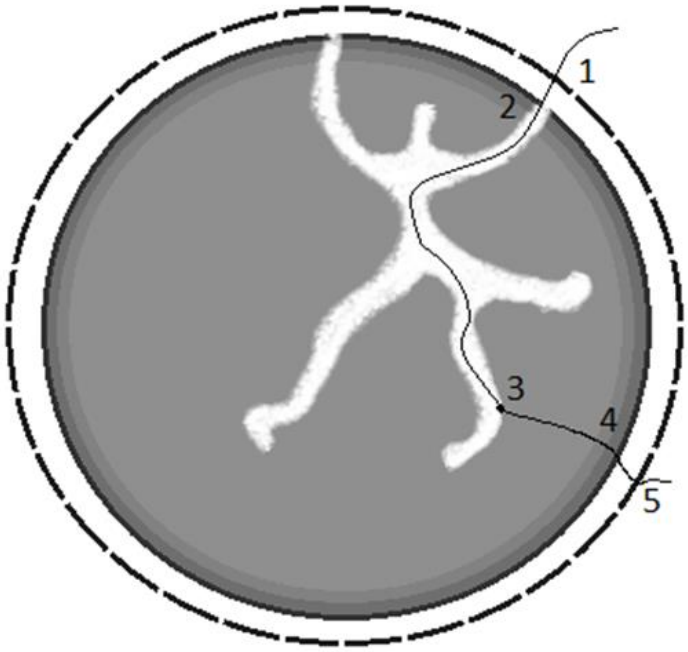

Figure 15: Phenomenology of mass transport (adapted from [30])

In contrast to the heat transport in the liquid phase, which can be neglected due to the high heat capacity of the surrounding liquid, this is of great importance in gas phase adsorption. [23, 26]

In gas phase adsorption, diffusion through the pores in the interior of the particle is usually the speed-determining step. In the case of adsorption from the liquid phase, however, the external diffusion often has an influence. [23, 26]

2.5.4 Dynamics of adsorption

The combination of kinetics and thermodynamics results in the adsorption dynamics. This becomes visible with the help of so-called breakthrough curves and thus serves the design of adsorbers. However, the dynamics also depend on the respective boundary conditions, such as process control and adsorber type. [34]

Ideally, a coupled concentration and loading front moves through the adsorber. The corresponding profiles are shown in Fig. 16. However, this does not usually occur, as such a profile changes greatly during adsorption.

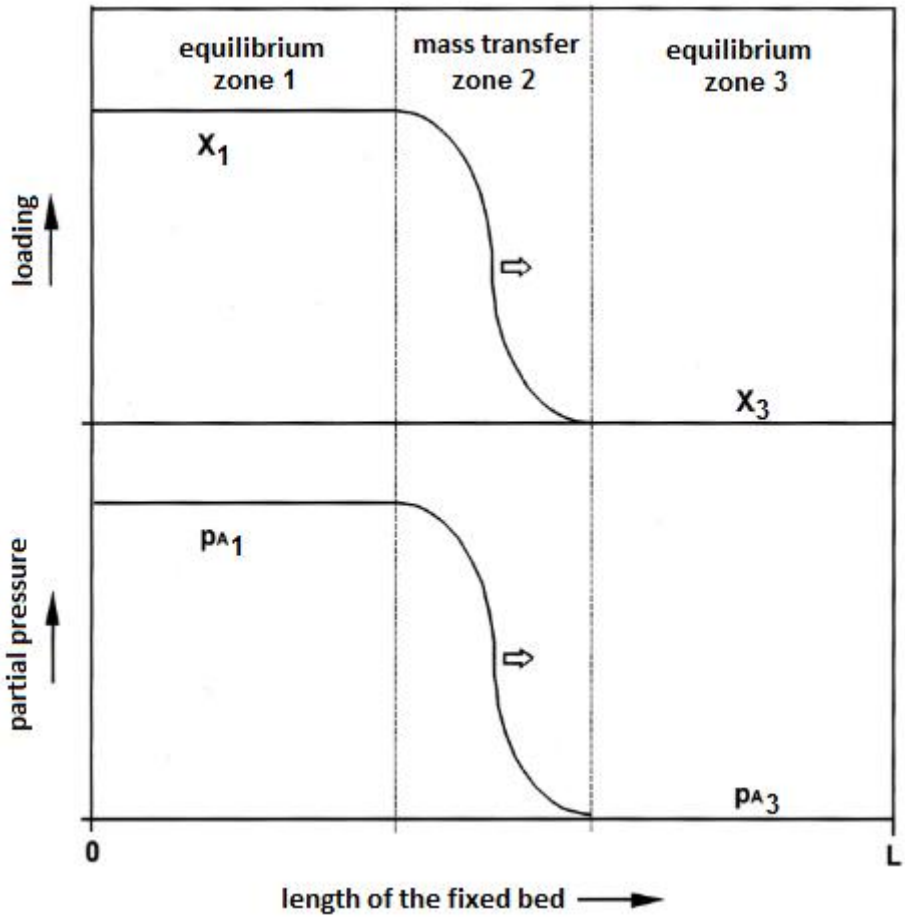

Figure 16: Concentration and loading profile in an adsorber (adapted from [34])

According to the isothermal equation, the adsorbent in the 1st zone is completely loaded with adsorbate. The partial pressure of the adsorbate in the gas phase is equal to the value of the carrier gas when entering the adsorber. If the process is carried out too long, this zone takes up the entire adsorber and the loading at the inlet corresponds to that at the outlet. [34, 37]

The transfer of the substance to be removed from the fluid to the adsorbent thus takes place in a zone in which the concentration of the adsorbent is reduced from the entry value to the exit value. This zone is called mass transfer zone (MTZ). With continuous operation of the adsorber, this zone moves further and further away from the entry point and towards the exit. It displaces the 3rd zone, which is unloaded and occupies the complete adsorber at the beginning of the process, and finally reaches the point where the adsorbate can be detected in the escaping gas. [34, 37, 38]

The time at which the first adsorbate is measurable is called breakthrough. As soon as the concentration at the outlet is equal to that at the inlet, this ends the adsorption cycle. The adsorbent is saturated and needs to be regenerated. The change of the concentration of the adsorbate in the tail gas over time is called the breakthrough curve and is shown in Fig. 17. The time t_b elapsed before the breakthrough is called the breakthrough time. t_h is the half-life and t_s is the time to complete saturation. c_o stands for the concentration of the adsorbate at the outlet and c_i for that at the inlet. [34, 37, 38]

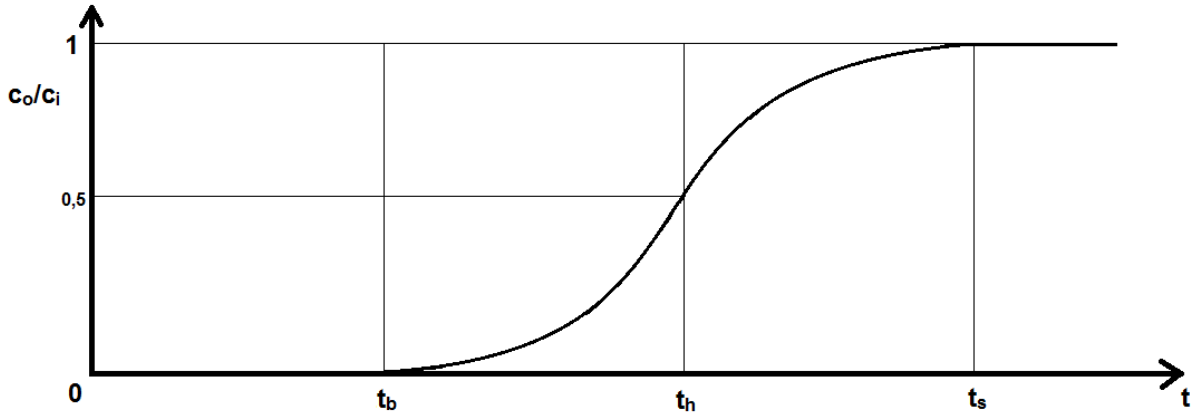

Figure 17: Breakthrough curve

Basically, it can be said that the separation of two substances works better the more different the adsorbability of the two substances is at the respective adsorbent. This depends on the physical and chemical properties of the substance and the adsorbent. In principle, it can be said that the substance with the highest boiling point is most strongly adsorbed in gas mixtures that are connected to an adsorbent. [39]

2.5.5 Desorption

The reversal process of adsorption is called desorption. This means that the particles pass from the surface of a material back into the fluid phase and the loaded, saturated adsorbent is regenerated. [34]

All desorption processes are based on the principle of the least constraint of LeChatelier. This means that the equilibrium of a system is shifted by the application of an external force in such a way that the system evades the force and its effect is minimised. In the case of desorption, an external constraint causes the thermodynamic equilibrium to shift in the desired direction between the loading of the adsorbent and the concentration of the adsorbent in the fluid. [34, 35]

Since adsorption takes place preferably at high pressures, low temperatures and high adsorptive concentrations in the fluid phase, desorption can be carried out primarily in three ways: [34, 35]

1. Increase of temperature > TSA - **T**emperature **S**wing **A**dsorption
2. Reduction of pressure > PSA – **P**ressure **S**wing **A**dsorption
3. Change in the composition of the fluid phase > CSA – **C**omposition **S**wing **A**dsorption

The TSA was part of the experiments carried out for this work. It is the most common method for the regeneration of adsorber fixed beds, where the adsorption is characterised by a high adsorption enthalpy, i.e. a strong interaction between adsorbent and adsorbate. This applies to almost all drying processes and exhaust gas purification methods since the low pollutant concentrations in the exhaust gas required in this case can only be achieved by strong interactions. [34]

In order to carry out the desorption it needs thermal energy. This energy can be supplied in different ways. The most common method is purging with inert gas or steam. Heat can also be supplied by heating elements, the introduction of electricity or by irradiation with microwaves or infrared radiation. [33]

By increasing the temperature, the load equilibrium shifts to lower values, see Fig. 18. The difference of the load (X_1 - X_2) is transferred to the gas and must be flushed out. After the bed has cooled down to adsorption temperature, it has pre-load X_2. Further flushing with adsorbate-free gas can also reduce the load. [33]

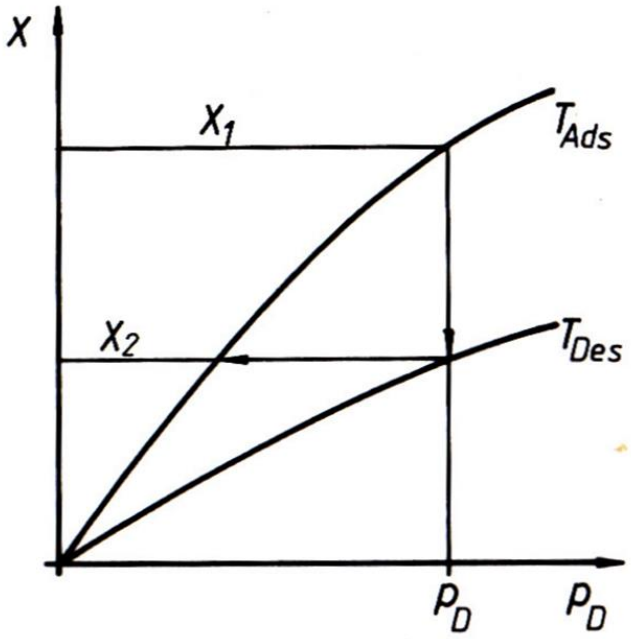

Figure 18: Dependence of the load on the temperature [33]

2.5.6 Adsorbents

The choice of the adsorbent and the determination of the operating conditions depend crucially on the adsorption equilibrium. Without knowledge, the efficiency of an adsorption process cannot be estimated. Since, in contrast to vapour/liquid equilibria, there are hardly any general prediction methods for adsorption equilibria, these must be determined experimentally. [36]

Basically, a distinction is made between the hydrophobic carbonaceous adsorbents such as activated carbon, coke and carbon molecular sieves and the hydrophilic inorganic adsorbents such as zeolitic molecular sieves, aluminium oxide and silica gel. All these adsorbents have a large specific surface area (> 100 m²/g). The inner surface is mainly created by the very fine micropores. These also represent the adsorption capacity since the pollutants preferably accumulate here. The wide macropores serve the fastest possible transport of the adsorbate into the interior of the sorption. [33, 36]

2.5.6.1 Activated carbon

Since the adsorbent used in these experiments was activated carbon, this is discussed in more detail here.

Activated carbon is produced from carbonaceous raw materials such as peat, wood, lignite, hard coal and nutshells. Two processes are used for production and activation: [40]

- Gas activation
- Chemical activation

Gas activation:

A moulded body is first produced from the raw material and then activated by partial gasification with steam or carbon dioxide at 700 – 1000 °C. The starting material and the duration of the steam or gas influence determine the pore size and distribution. The activated material is pyrolysed in a furnace at about 800 – 900 °C in an inert gas atmosphere and then crushed (if it is granulated), sieved and packaged. [33, 40]

Chemical activation:

This is mainly used to produce powdered coal. The raw material, e.g. wood first dried and then mixed with dehydrating chemicals such as zinc, calcium, magnesium chloride or phosphoric acid. It is then heated to 400 – 800 °C in an airtight oven. The dehydrating atmosphere causes hydrogen and oxygen atoms to be removed from the material and at the same time activation and carbonation take place. It is then cooled with diluted phosphoric acid, washed out and separated. Finally, the coal is dried and pulverised. [33, 34, 40]

2.6 Gas chromatography

Gas chromatography (GC) is a method that can be used both to obtain pure substances and to perform quantitative and qualitative analyses of mixtures. For this purpose, the individual components must first be separated. This is done using a gaseous and a solid or liquid phase. The process can be controlled by means of the temperature. Only compounds that are sufficiently volatile or vaporisable at higher temperatures without conversion or decomposition can be analysed by gas chromatography. [41]

2.6.1 Build-up and function

Basically, a gas chromatograph consists of a gas reservoir (1), an injector (2), a separation column (3) in the GC oven, a detector (4) and a unit for signal recording and output (5). Schematically shown in Fig. 19 [42].

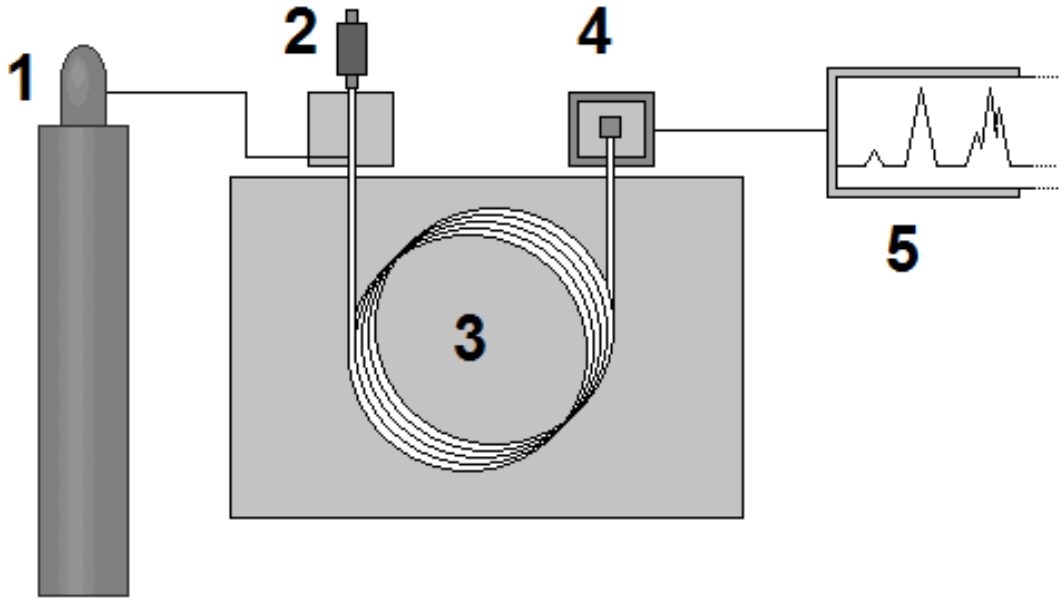

Figure 19: Schematic diagram of a gas chromatograph

The gas reservoir is a tank that contains the carrier gas. Mostly helium, hydrogen, or nitrogen. This gas is called mobile phase and is responsible for transporting the sample through the separation column. The substance to be analysed is introduced into the pressurised inert carrier gas by means of a microlitre syringe or a multi-way valve and a sample loop. If it is a liquid, it is usually first evaporated. However, there is also the possibility of adding the liquid sample to the column itself without prior external evaporation. This procedure is called on-column injection. [41]

After evaporation and mixing with the carrier gas, the sample enters the separation column. This column contains a solid stationary phase and can have either a solid (GSC = gas-solid-chromatography) or a liquid (GLC = gas-liquid-chromatography) consistency. Here starts the separation process. Due to the different intermolecular interactions between the components and the stationary phase, the components of the sample take different lengths of time to flow through the column and be detected by the detector. On the way there, the components repeatedly attach themselves to the stationary phase until saturation, are dissolved again, transported further and attach themselves again. These processes of settling and dissolving are called separation stages and can occur several hundred times in a single chromatographic separation. [41, 42]

The separation column is located in the column oven, the temperature of which can either be kept constant or programmed to be linear or non-linear with temperature-constant periods. [41]

The columns generally differ in the efficiency of the separation, the selectivity of the stationary phases and the quantity of compounds that can be separated in them. In addition, there are differences in the types of support surfaces on which the stationary liquid is located, i.e. whether it is a capillary or packed column; further, in the geometry, i.e. diameter and length, and the amount of effective stationary phase contained in a column. [41]

How quickly and how completely even chromatographically very similar components of a mixture can be separated and detected is determined by the efficiency of the separation achievable with a particular chromatographic column. It is also important here that the most important parameters such as carrier gas flow and temperature are optimised so that only short retention times (analysis times) are required despite high efficiency. [41]

The components separated in the column enter the detector with a characteristic concentration profile in the carrier gas. Depending on the analytical goal to be achieved, the detector shows all or only some representatives of certain substance classes specifically, generating a more or less intensive signal. [41]

A computer program then outputs the data obtained in the form of a digital chromatogram. This is an analysis report with numerical values, i.e. with figures for the positions and areas or heights of all or certain peaks. A peak is the characteristic concentration profile of the individual separated components. Figure 20 shows such a chromatogram.

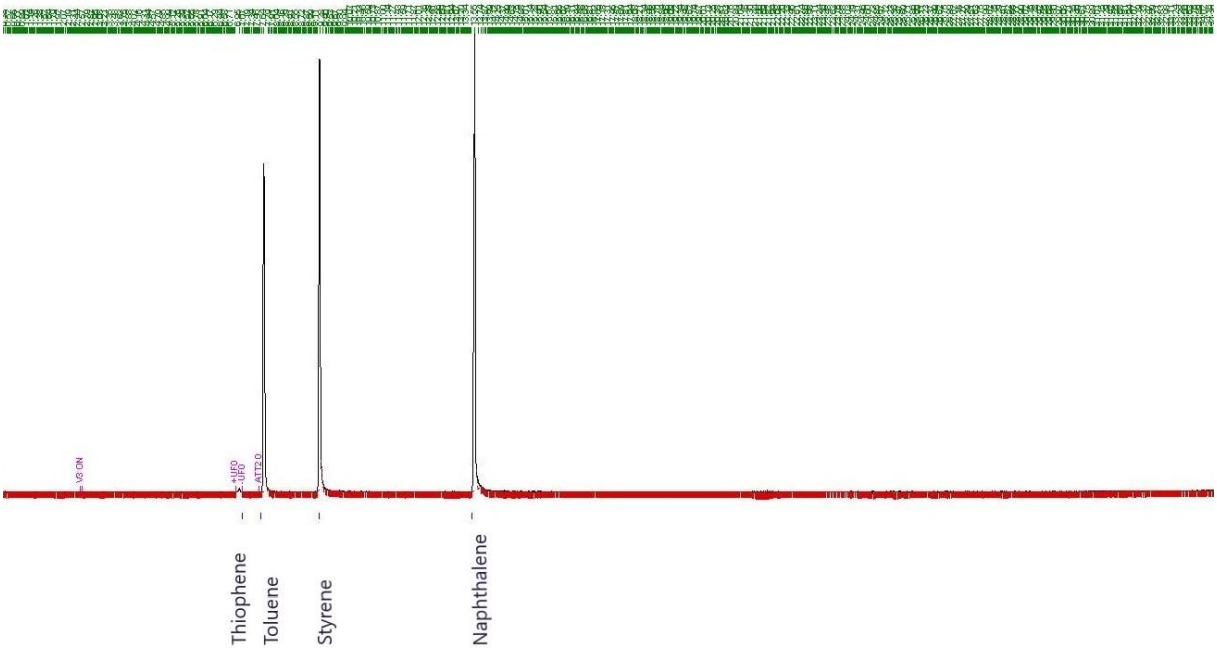

Figure 20: Chromatogram with peaks of Thiophene, Toluene, Styrene and Naphthalene

3. Design of experiments

The aim of these experiments was to find out whether activated carbon as a TSA can be used to remove the tars from the product gas of a biomass gasification plant and thus, be used instead of a cold biodiesel scrubber. As the different tars serve as the basic components of many chemical products, they are to be separated from each other in order to make them economically usable. The tar composition with which the experiments were conducted corresponds to the composition after a hot RME scrubbing process.

The experiments were carried out in an oven that was modified for this purpose. This was originally located in the premises of the company BEST (formerly Bioenergy 2020+) in Güssing (since its relocation in autumn 2019 in Simmering). The entire setup is shown in Figure 21. In the upper left part of the picture one can see the pressure regulator. This was used to control the addition of nitrogen, which was the carrier gas for the tars, into the sample loop. Furthermore, an injector was installed, which was responsible for the injection of the tars. In the lower mid part of the picture, the pump is visible, which introduced the mixture of substances into the exhaust pipe after the GC. In addition, two washing bottles were mounted, one is visible next to the pressure regulator and one outside the oven. Both contained isopropanol as solvent. A bypass led through the bottle next to the oven, so that in case of desorption, excess tar was collected there. The second was downstream of the GC and was intended to protect the pump and the exhaust pipe from tar condensation.

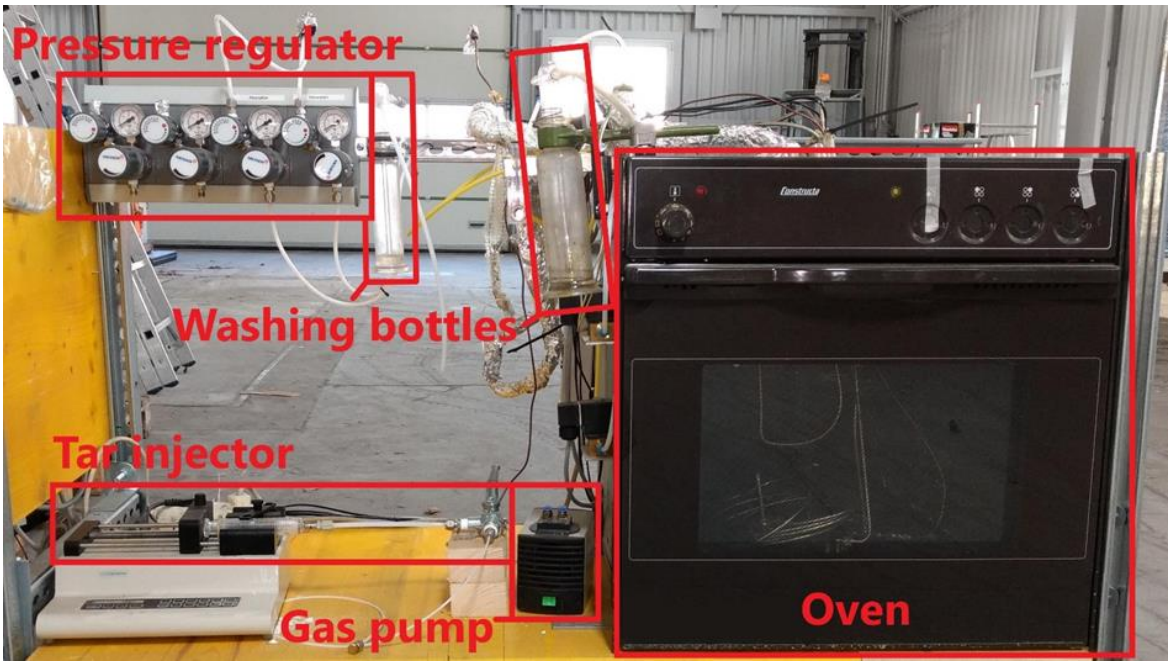

Figure 21: Experimental setup

Through a thin tube (6mm, ID: 4mm), the gas mixture passed through the ceiling of the oven and into an evaporation column, where the sample was quickly and completely evaporated. Connected to the column was a reactor which contained the activated carbon that bound the tars to itself during the adsorption phase. The desorption phase

was initiated by raising the temperature in the oven, which caused the tars to dissolve and migrate through a tube further into the gas chromatograph. Furthermore, three temperature measuring units and a flushing pipe were installed in the oven. If the tars had escaped from the oven, the flushing line would have flooded the oven with nitrogen and thus freed it from the undesirable components. Figure 22 shows the structure inside the oven.

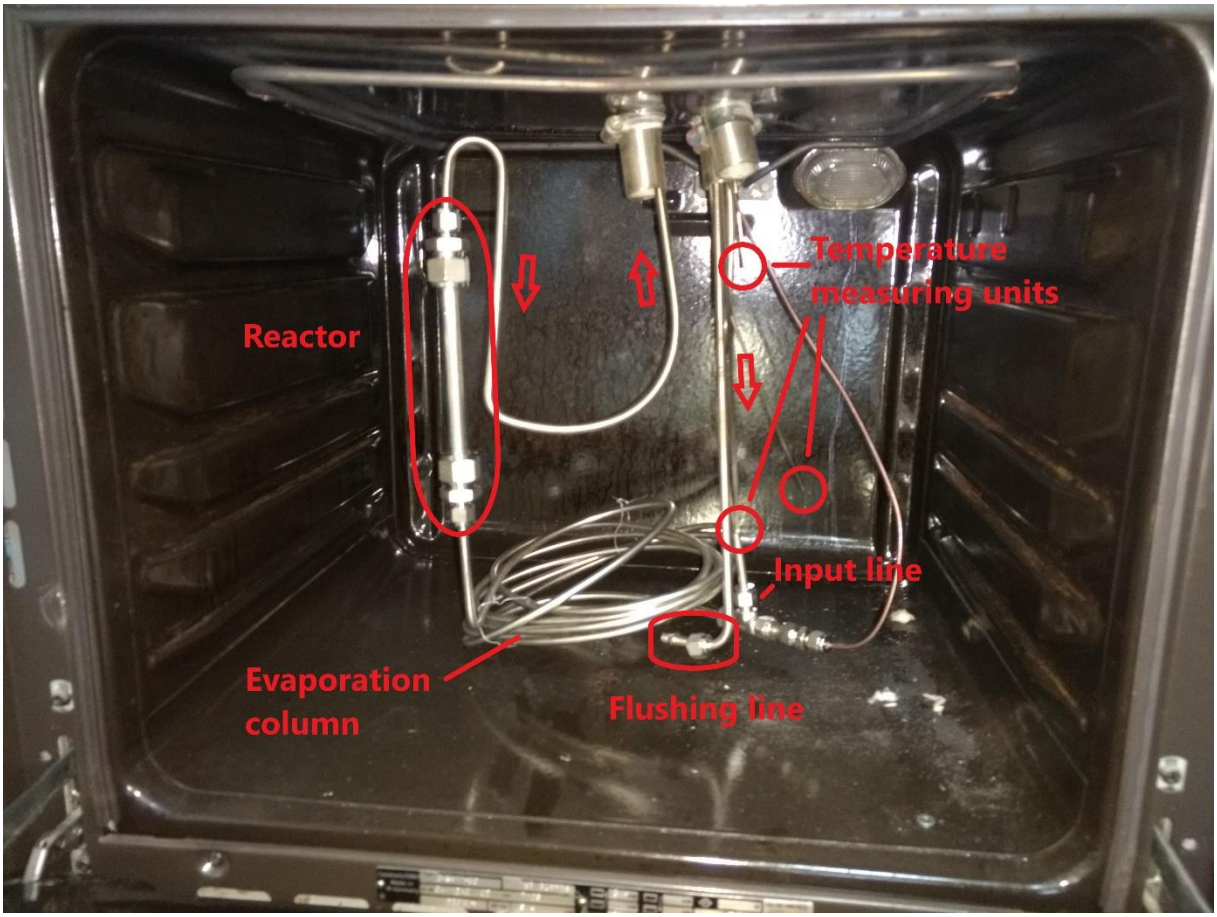

Figure 22: Interior view of the modified oven

The gas chromatograph used here was the "Clarus 500" from PerkinElmer, equipped with an FID (flame ionisation detector), see Figure 23. The gas mixture, after passing through the oven into the GC, was separated into its individual components by a separation column and finally recorded by the detector.

Figure 23: Gas chromatograph used for the experiments

The separation columns for the experiments were made by the company Restek. For the tests 1 to 3 the MXT-1 was used with a length of 60 m, an inner diameter of 0.53 mm and a film thickness of 0.25 µm. In this version the stationary phase consists of 100% dimethylpolysiloxane. The MXT-5 was used for experiments 4 to 6. This has the same specifications, but the stationary phase here consists of only 95% dimethylpolysiloxane and 5% diphenylpolysiloxane. Figure 24 shows the interior view of the GC including such a separation column. The data recorded by the GC were finally output by the computer in form of value tables and chromatograms.

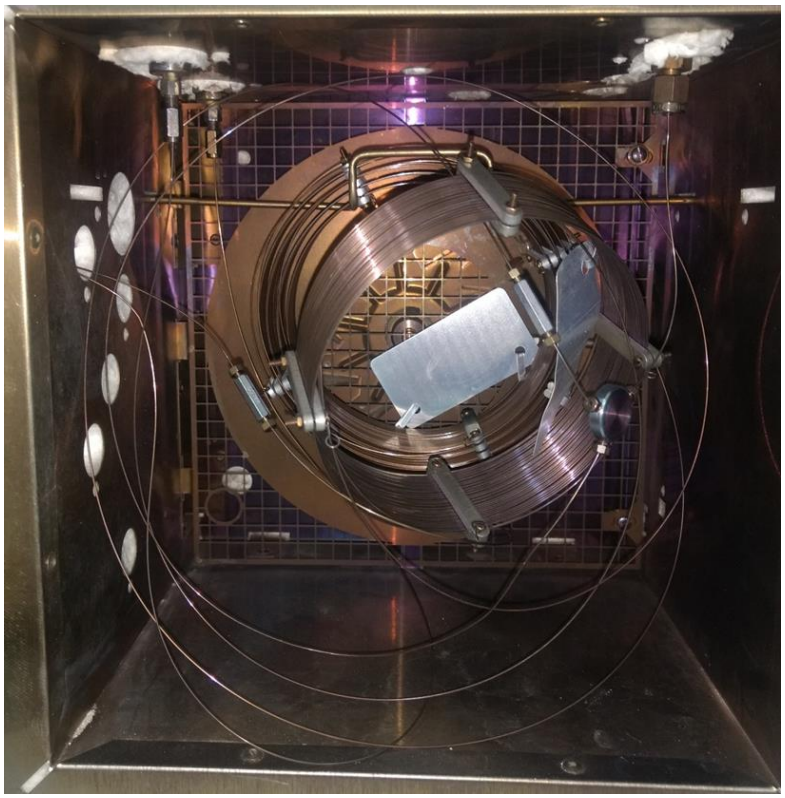

Figure 24: Interior view of the gas chromatograph with capillary column

4. Results and discussion

A total of six trials were conducted. The runs 1 to 3 were primarily aimed at determining the most suitable parameters in terms of gas flow/quantity and adsorption/desorption time. In experiments 4 to 6 only minor changes were subsequently made. Some process parameters did not change during the entire experiments. These include in the main the geometry of the adsorber. This had a diameter of 9 mm and an internal cross section area of 6.36173 * 10^{-5} m². Furthermore, the adsorption temperature was always in a range of 36 to 42 °C. For desorption, the temperature was increased to 180 °C in each case. The exception to this is trial 4, where desorption was carried out at 152 °C. The data of the tar mixture used are given in Table 4:

Table 4: Characteristics of the tar

Tar concentration	25 mg/l		
Tar flow rate	10 mg/min = 11.111 µl/min		
Density	900 mg/ml		
Tar composition			
Substance	[g]	[m-%]	[mg/m³$_{STP}$]
Toluene	815	83.75296	20,938.24
Styrene	83	8.52944	2,132.36
Naphthalene	72	7.39903	1,849.76
Thiophene	3.1	0.31857	79.64
Total quantity	973.1	100	25,000

4.1.1 First trial

The first trial was started on 27.03.2019 at 15:17 with a quantity of 3.52 g activated carbon in the adsorber. It was started with a temperature of approx. 40 °C. The tar mixture was first added at 16:30. As can be seen in Figure 25, thiophene in a quantity of about 35 g/m³ is initially detected by the GC throughout. However, due to the small amount of thiophene in the mixture, this must be a fault of the GC. Only during the second adsorption/desorption phase do these values take on an expected course, i.e. low values during adsorption and increased values during desorption. The first desorption phase was initiated after about 3 ½ hours, when the temperature was increased to 180 °C, which took 20 minutes. It can be seen that toluene and styrene, which were previously only detected in small amounts, are now much more detectable. For toluene, the amount detected is 95 g/m³, for styrene 55 g/m³. Thiophene reaches a value of 6 g/m³. Naphthalene was detected almost constantly at 4 g/m³ over the entire period of the first experiment and therefore it is excluded from this trial since the analyse obviously did not work properly. This could be due to a separation column unsuitable for this component, but since it worked better in the subsequent experiments, this was probably again a fault of the GC.

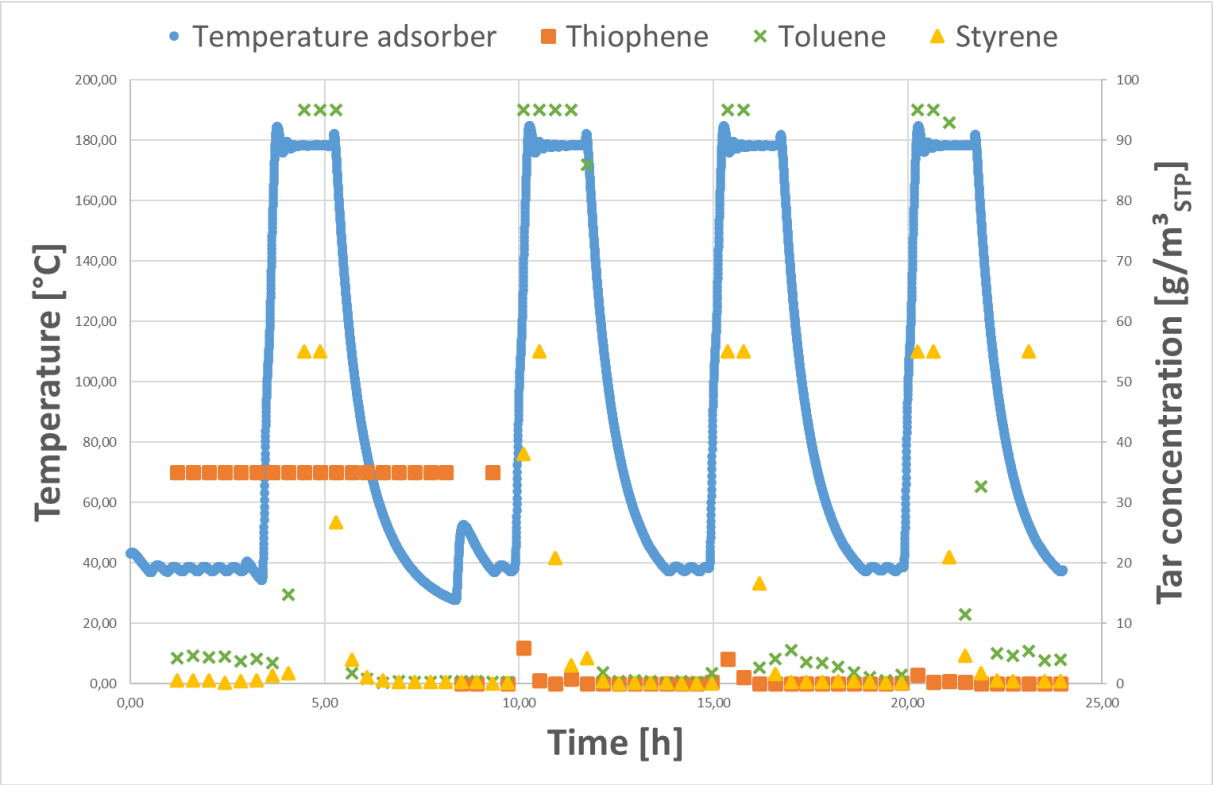

Figure 25: First trial, day one

Since the tar values, in contrast to the temperature, which was measured six times per minute, were measured only every 25 minutes, it is unfortunately not possible to say at which temperature the substances dissolve exactly or up to which temperature they adhere to the activated carbon. After 90 minutes the desorption was stopped, which meant that the components were again adsorbed by the activated carbon and were only detected to a very small extent. It took about two hours until a temperature of 40 °C was reached again. The long cooling time is due to the small oven. If it were a "non-laboratory scale" plant, it would be relatively shorter. After another 3 hours the temperature was increased again to 180 °C. This was again held for 90 minutes before it was lowered again. Afterwards, a duration of 90 minutes was also set for the adsorption. This rhythm was maintained for the entire experiment, which lasted until 01.04.2019 at 9:13 am. During the desorption phases on the remaining days, toluene and styrene consistently reach their peak values, but sometimes form very irregular peaks. Thus, it often happens that these substances drop to values close to 0 and suddenly show a maximum again in the next measurement. The maximum values of thiophene also vary very irregularly and are between 1.5 and 35 g/m³.

From 30.03.2019 at 21:30 there are unfortunately no further values for tars. This can be attributed to either a failure of the GC or the injection.

In summary, it can be said about the first trial that no equilibrium of the individual components with regard to adsorption and desorption had yet been established. For example, there were peaks in places where they should not occur or at a height that should not be possible. However, this may be related to the complications that occurred with GC. In general, as can be seen in Figure 26, which shows the second day as an example, tars dissolve to a high degree at increased temperatures.

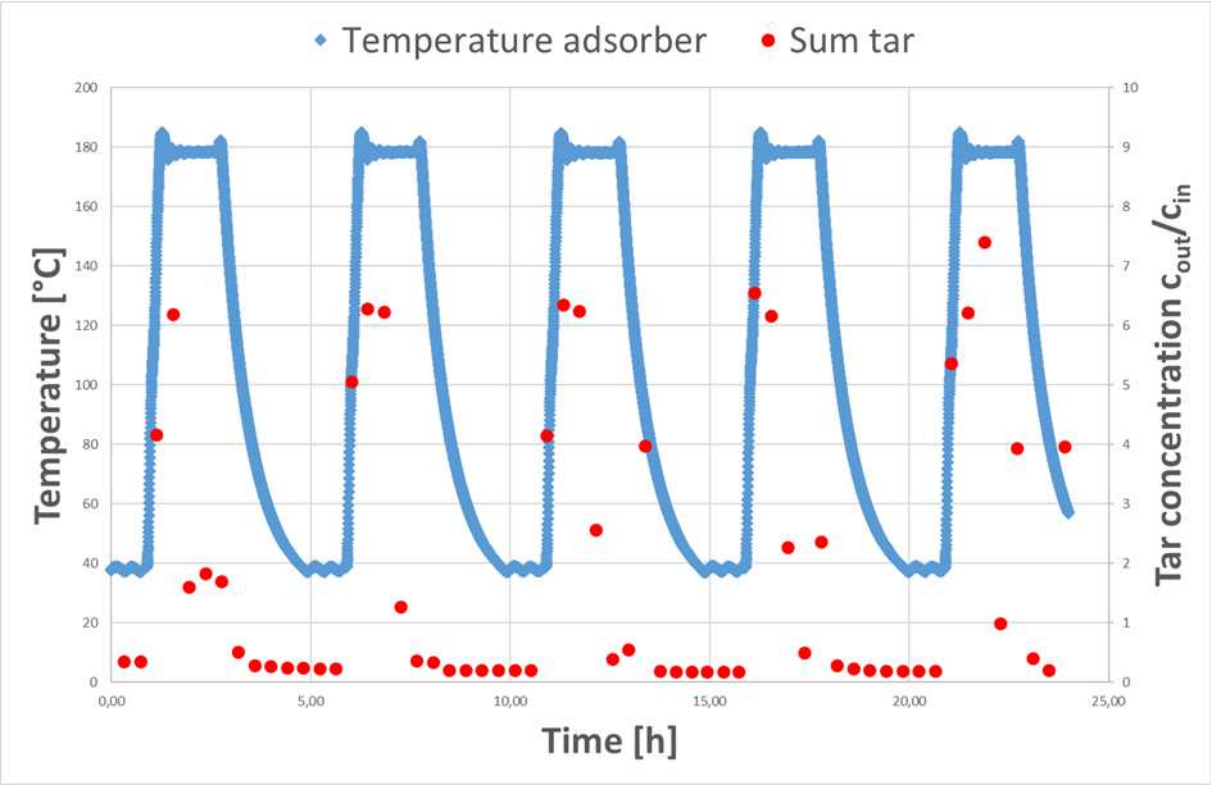

Figure 26: Overview of the tar concentration of all tars on day 2

4.1.2 Second trial

The second trial was started on 01.04.2019 at 12:53, with an activated carbon quantity of 3.48 g. At 13:58 tar was injected for the first time. Figure 27 shows the first day of this experiment. In contrast to the first experiment, no constantly high values of one of the substances were measured at the beginning, but, as it should be during the adsorption phase, only very low values. In the first desorption phase, thiophene and toluene are immediately dissolved. The other two substances, styrene, and naphthalene, however, do not. What can be seen at first glance on day 1 and does not change during the other days, is that the peaks of the individual substances are all slightly shifted backwards in time in relation to the temperature peaks. This is probably due more to a problem with the GC than to an actual desorption of the substances, which only takes place after a certain holding time of the elevated temperature.

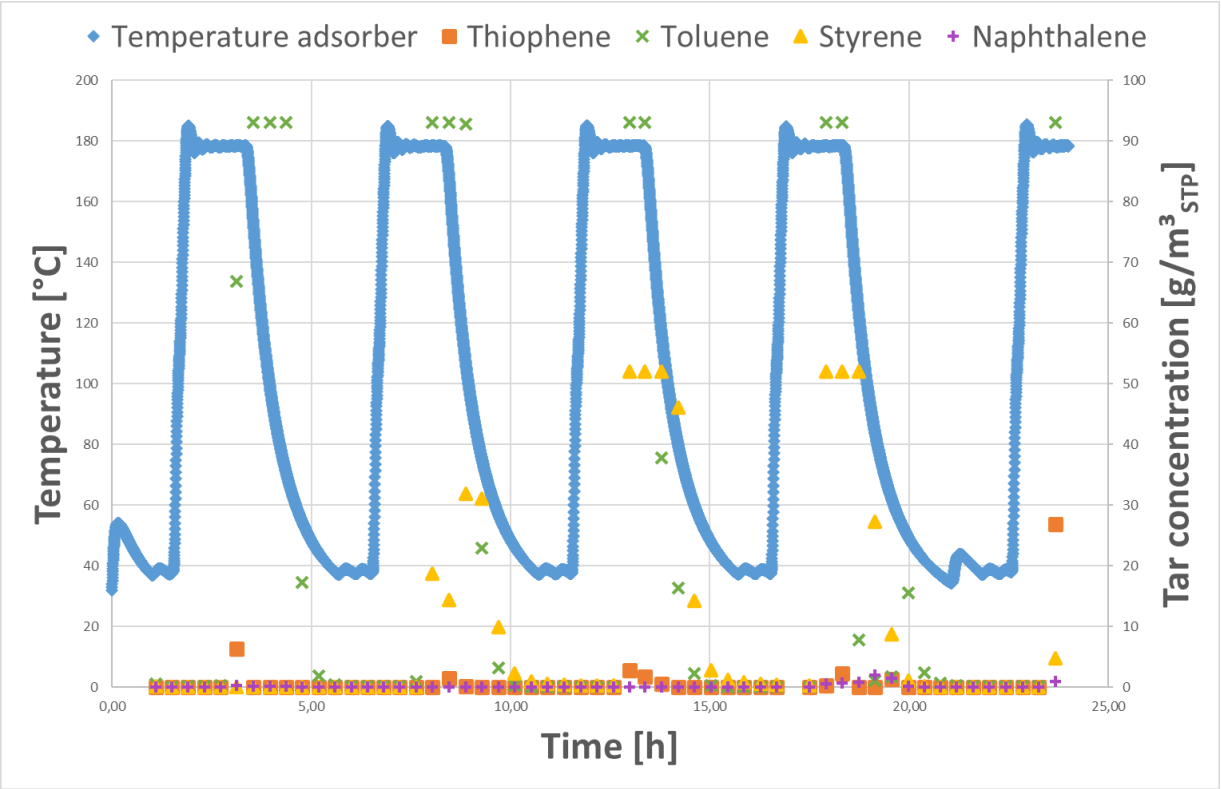

Figure 27: Second trial, day one

For desorption, the temperature was increased to 180 °C throughout the entire experiment and was maintained for 90 minutes at the beginning. In general, the heat-up phases lasted another 20 minutes and the cool-down about 120 minutes. In Figure 27, it appears that the adsorption phases lasted only 70 minutes, but this was not the case. Tar was injected for 90 minutes. However, since the cooling phase before that took so much time, the tar injection was started before 40°C was reached. It can be seen that from the second desorption phase onwards, styrene is also dissolved and from the fourth phase onwards also naphthalene.

The adsorption phase following the fourth desorption was extended to about 130 min and the subsequent desorption to 180 min. It can be seen that the values of the components, with the exception of naphthalene, do not dissolve at all over the entire duration, but drop again after about half of the time. This can be seen right at the beginning in Figure 28, from which it can be concluded that such a long desorption phase is not necessary, despite the fact that adsorption has been carried out for a longer time beforehand, in order to remove the substances from the activated carbon as completely as possible.

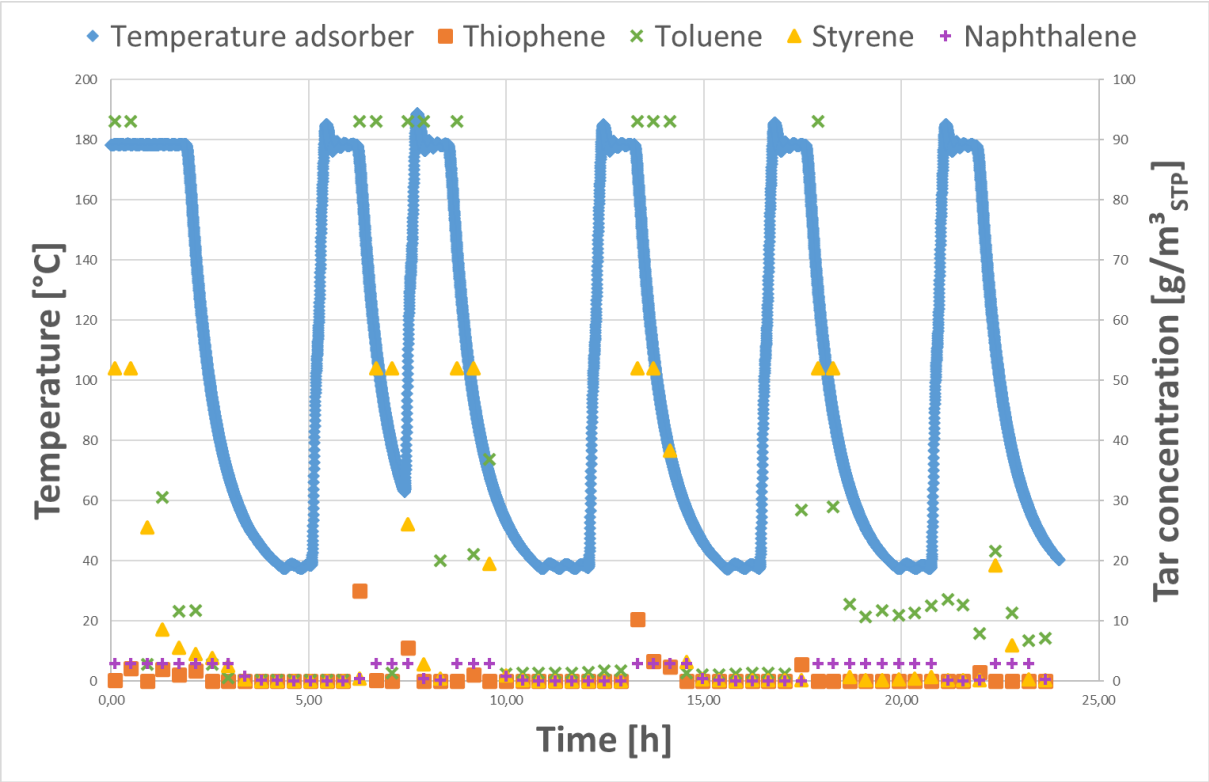

Figure 28: Second trial, day two; right at the beginning during the first desorption, it can be seen that the values drop again early. Afterwards two directly consecutive desorption phases.

After another 90-minute adsorption phase, two desorption phases of 50 minutes each were run directly one after the other, with the temperature in between only being reduced to 61 °C for a short time. Due to the shift of the tar values in relation to the temperature, mentioned at the beginning, it is somewhat more difficult to interpret this section. In principle, all tars are released from the activated carbon in this phase. Thiophene and toluene are released a little earlier than the other two components. By lowering the temperature, the amount of detected tars is immediately reduced to a minimum. Unfortunately, it is not possible to determine at what temperatures this happens. The rapid increase in temperature also causes a rapid rise in tar values. With the exception of thiophene, which during this "double desorption" forms three peaks, each with descending peak values, the other components each reach their maximum values. For toluene these are 93 g/m³, for styrene 52 g/m³ and for naphthalene 3 g/m³. It should also be mentioned that the latter, although it has low peaks, is broader, i.e. longer lasting than the other substances. This can also be observed on the other days of this experiment. For the remaining day, the desorption time was maintained at 50 minutes, and the adsorption time at 90 minutes. After the last desorption of this day the gas flow rate was changed. Only for the adsorption it was maintained at 0.4 l/min, during the remaining cycles it was increased to 1 l/min. What can already be seen during the last adsorption phase of this day is that the toluene no longer drops to its previous minimum but is also continuously detected here with an amount between 5 and 15 g/m³. This behaviour can be observed during the whole **third day**, see Fig. 29. The remaining days in a weakened form. This is probably due to an overload produced during the last TSA cycle of the second day (Fig. 28). The TSA is slowly recovering from this. The increased gas flow rate can be ruled out because it was

increased only shortly after the first appearance and was not maintained as long as this phenomenon occurs.

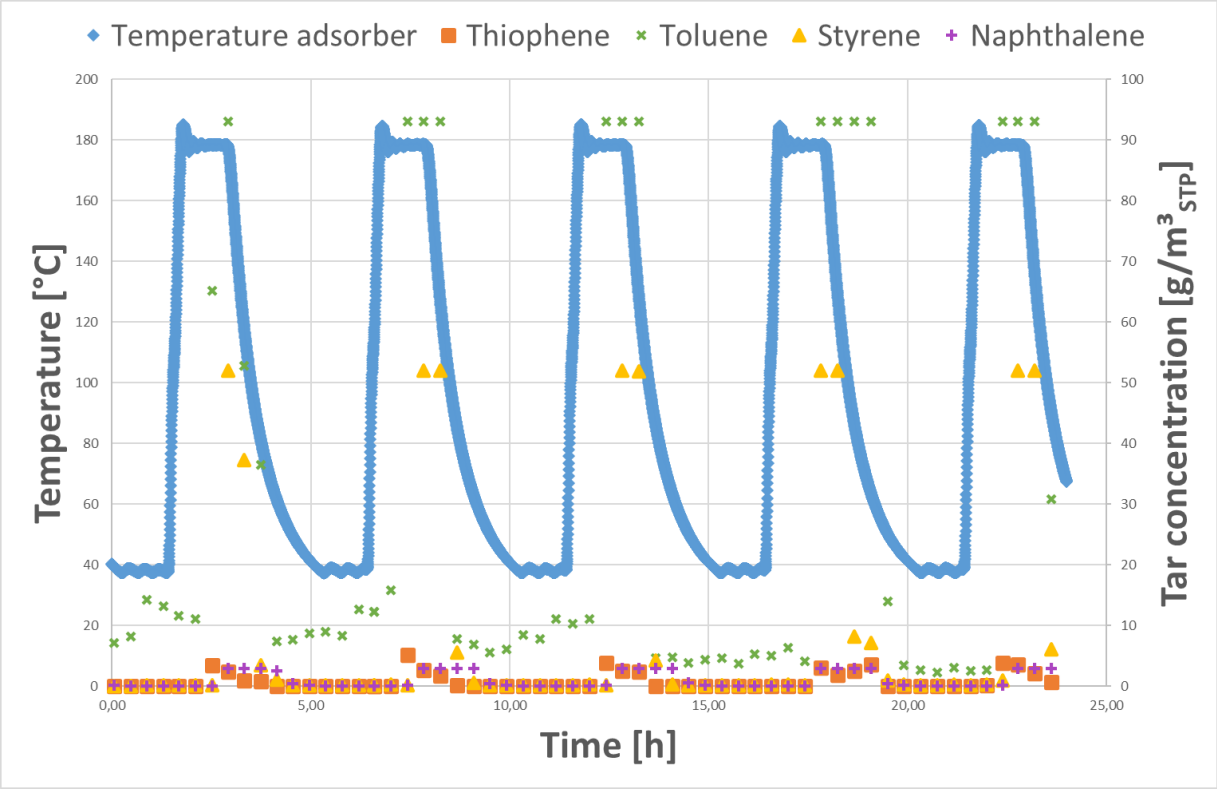

Figure 29: Second trial, day three

For the **third, fourth and fifth day**, the times for desorption were set at 70 minutes and for adsorption at 90 minutes. In addition to naphthalene, toluene also forms wider peaks during this time, and on the fifth day also styrene. Apart from that, no further special features can be identified for these three days.

At the beginning of the **sixth day** the desorption time was increased to 90 minutes. It is worth mentioning that from this day on naphthalene is detected almost continuously with a quantity of 3 g/m³.

The **seventh day**, also the last day with tar values, shows surprisingly high peaks of thiophene during desorption. These are in the range between 18 and 40 g/m³. The toluene never drops below 6 g/m³ during the whole day and the styrene also forms wider peaks than usual. The reason for this behaviour could be an overload of the activated carbon. The continuous load of the previous days, the constant raising and lowering of the temperature and the pollution by the tars could be responsible for this. The trial was finally stopped one day later, on 09.04.2019 at 15:11.

The fourth day serves as an overview of the overall behaviour of the tars, see Fig. 30. It is again very nice to see how the tars dissolve during desorption and are adsorbed again when the temperature is lowered. It can also be seen that the outlet concentration of tars decreased to 4 to 6-fold compared to the first experiment, where it was between 6 and 8-fold of the inlet concentration.

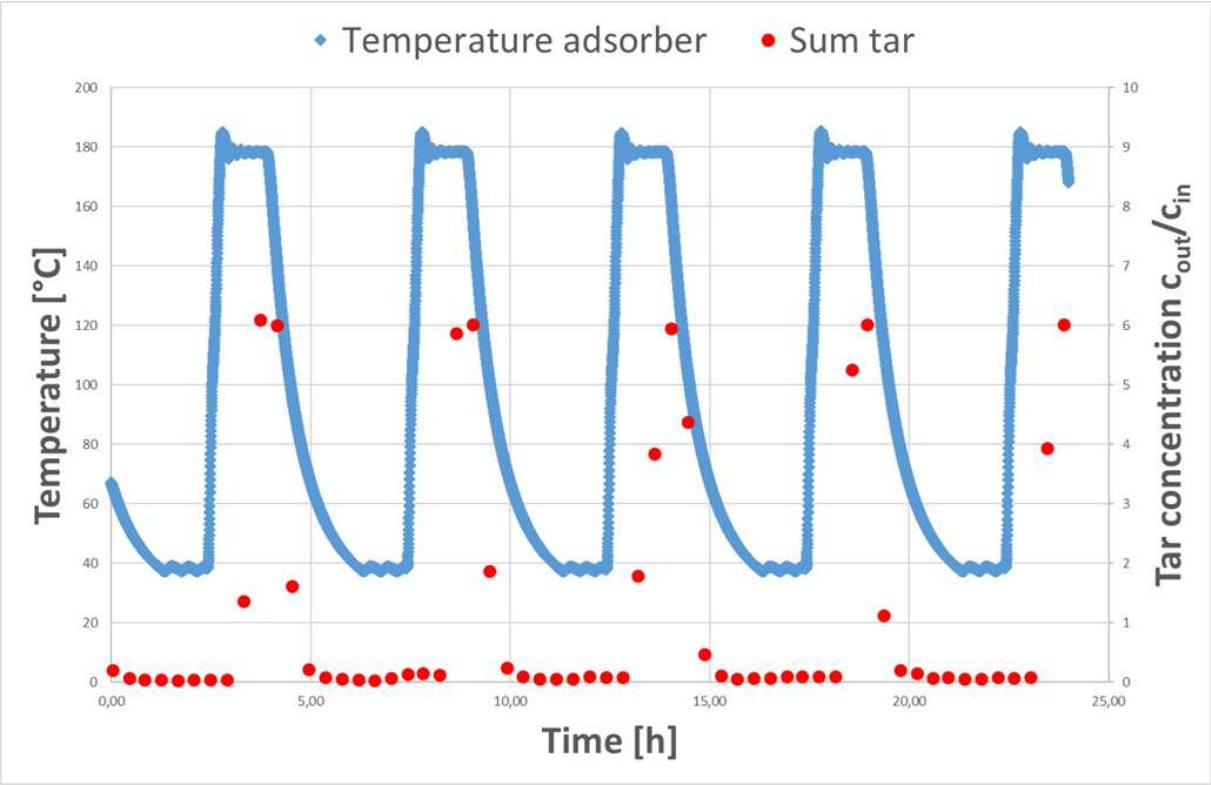

Figure 30: Overview of the tar concentration of all tars on day 4

The most important finding from this experiment is that desorption phases longer than the preceding adsorption are by no means necessary. For example, after a 130-minute adsorption, a 180-minute desorption was performed, but after about half the time no more substances were dissolved. From this it can be concluded that about 70% of the adsorption time is already sufficient for a successful desorption.

Apart from that it can be stated that the substances form, following the temperature curve, nicer peaks compared to the previous trial. Of particular note here is naphthalene, which was previously detected almost continuously in increased concentrations.

4.1.3 Third trial

In this trial for the first time, the times for adsorption, desorption, heat-up and cool-down were determined at the beginning and not changed. The same applies to gas flow and quantity. These values were then also adopted and retained for tests 4 to 6. Table 5 provides an overview:

Table 5: Overview of the duration and gas flow of the various phases

	Time [min]	Gas flow [l/min]	Gas volume [l]
Adsorption	90	0.4	36
Heat-up	20	0.2	4
Desorption	90	0.2	18
Cool-down	120	0.2	24

The third trial was started on 25.04.2019 at 15:58, with the tar mixture being added for the first time at 16:27. The temperature was measured only once per minute from this run. And in contrast to the first two trials, the tar values were only measured about every 35 minutes, which was necessary to obtain a stable GC measurement. The values assume the typical course right at the beginning and remain the same during the entire **first day**. However, the peaks are significantly lower compared to the previous tests. Thus, toluene only reaches a maximum of 43 g/m³, styrene 12.2 g/m³, thiophene 0.82 g/m³ and naphthalene 1.8 g/m³. However, the latter shows an atypical course. Thus, the values are almost continuously above 1 g/m³ and decrease just at the transition from adsorption to desorption.

At the beginning of the **second day** there was either a failure of the GC or tar injection. This continued until the end of the **fourth day**, so no data are available for this period. On **day five**, the components regain their peaks during the first two desorption phases, but not to the same extent as before. The behaviour of the naphthalene does not change from before either. After that, there was another failure of the GC, lasting about five hours.

Unfortunately, there were also repeated failures during the following days. This happened for about eight hours on the **seventh day** and for about three hours on the **eighth**. Furthermore, no data is available for the entire **tenth day** and the first 17 hours of the **eleventh day**. For the times for which data are available, the picture is similar to that at the beginning of the experiment. Toluene continues to form the strongest peaks, with a quantity of 43 g/m³ each. The values for styrene are always between 4 and 15 g/m³ during the desorption phases, for thiophene at max. 4 g/m³. Also, the behaviour of naphthalene does not change compared to the beginning. All this can be seen as an example in Fig. 31, which shows the ninth day.

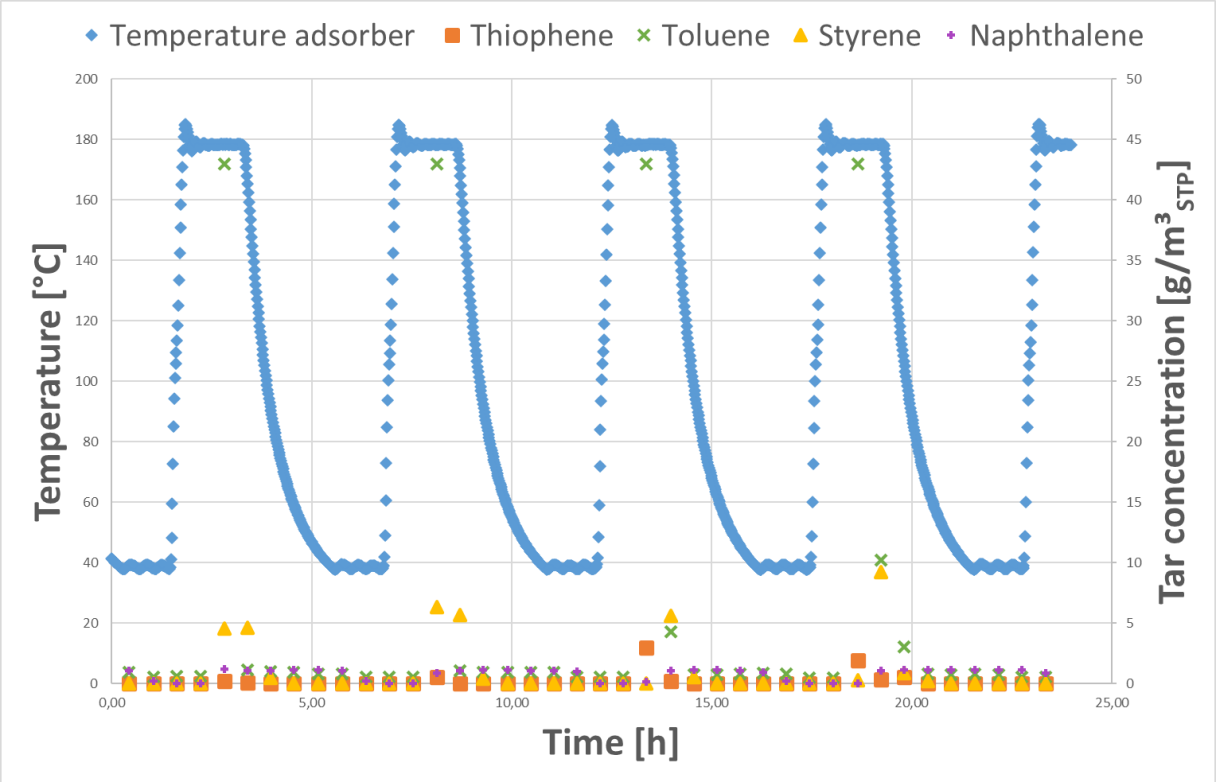

Figure 31: Third trial, day nine

On the last day, the **twelfth day**, only toluene formed peaks, which were rather small with 10 g/m³ and below. The trial ended on 07.05.2019 at 06:59.

Due to the many failures and the associated lack of data, it is unfortunately not possible to obtain any precise findings from this experiment. Only the much lower amount of detected tars, i.e. lower peak values, during the desorption phases is worth mentioning. This is also reflected in Fig. 32, which shows an example of the sum of tars on the sixth day. The tar concentration during desorption in this experiment is on average only 2.

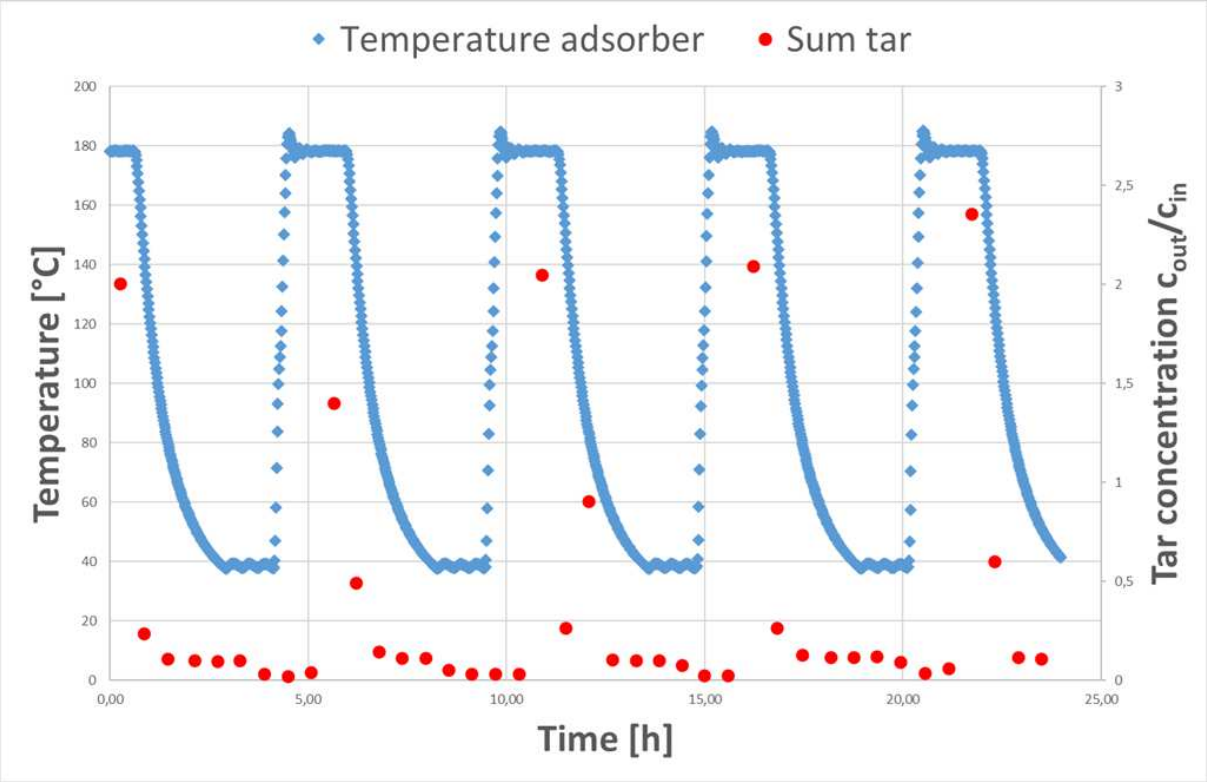

Figure 32: Exemplary overview of the tar concentration of this trial on day 6

4.1.4 Fourth trial

This attempt was by far the longest and lasted 23 days. In order to minimise the problems of the previous runs, firstly the separation column was changed and secondly the GC measurements were only carried out every 53 minutes. The trial was started on 18.06.2019 at 21:03 with 3.76 g of activated carbon. The tar mixture was first detected at 21:29. The duration of the individual phases can be seen in the previously mentioned Table 5. In contrast to the previous experiments, the temperature for desorption was only increased to 152 °C instead of 180 °C.

The **first day** was used to calibrate and check the equipment used. Thus, a temperature of 120 °C was started and maintained for 10 hours. Afterwards, the usual adsorption/desorption phases were started. During desorption substances toluene, styrene and naphthalene immediately reached peak values of 35, 13 and 5 g/m³. Thiophene was detected with a quantity of 3.3 g/m³. The three first-mentioned substances maintain this behaviour, with the exception of individual variations, also over the next three days. Merely styrene shows peak values in the range of "only"

8 to 10 g/m³ on the **second day**. It is also worth mentioning that during this period the values of toluene never drop below 1 g/m³ during the adsorption phases, i.e. this component is never adsorbed by the activated carbon to the usual extent as the other substances or as was always the case in the previous tests. The peaks of thiophene are subject to relatively strong variations, they vary between 0.3 and 3.1 g/m³. Furthermore, it can be seen, that thiophene and toluene reach their peaks one measurement before styrene and naphthalene, i.e. presumably dissolve from the activated carbon a little earlier. However, due to the large time intervals between the individual measurements, it is unfortunately not possible to determine this period more precisely. Only from the sixth day onwards the peaks "emerge" at the same time. As already partly noticed in the previous experiments, naphthalene shows “wider" peaks, which indicates a longer desorption of this substance. Fig. 33 serves as an example for all these findings.

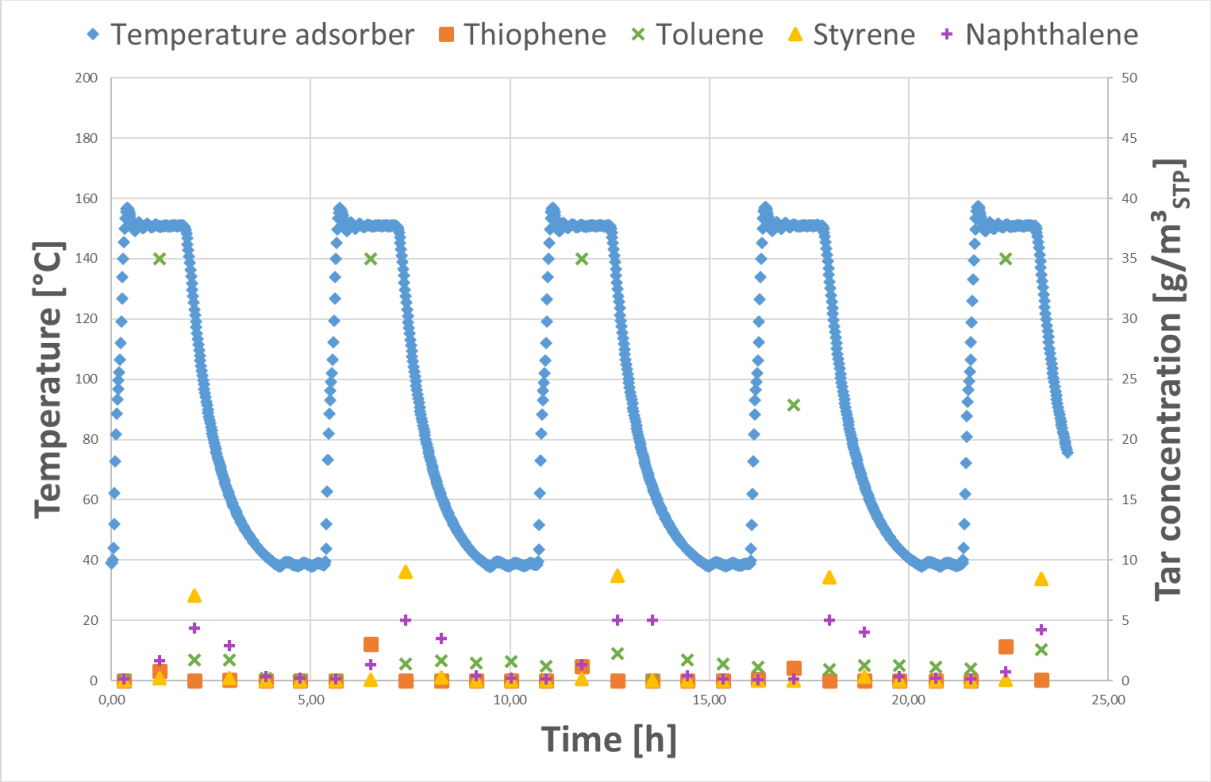

Figure 33: Trial 4, day 2: Thiophene and toluene reach their peaks noticeably earlier than the other two substances. In addition, the " wider" peaks of naphthalene are visible.

From the second desorption of the **fifth day**, the peaks of naphthalene decrease a little and those of styrene decrease significantly. For styrene, they then vary between 0.1 and 5 g/m³. On the **seventh day** they increase again and from the **eighth day** on a certain constancy is reached. The peak values of styrene, for example, range from 3.8 to 4.7 g/m³ and those of naphthalene from 1.5 to 2.2 g/m³. From this point on, thiophene is only detected to a very small extent during the desorption phases and does not exceed the value of 0.35 g/m³ until the thirteenth day. Only then does it rise again in a few cases up to 0.8 g/m³. Toluene remains unchanged during this period.

At the end of the **ninth day**, the peaks of all components break down significantly, the most striking of course is with toluene. Unfortunately, it is not clear what this is due to.

From the middle of the following day on, the components resume their original course and remain so until the end of the **thirteenth day**. Interestingly, styrene, like naphthalene, forms wider peaks from this point on. See Fig. 34.

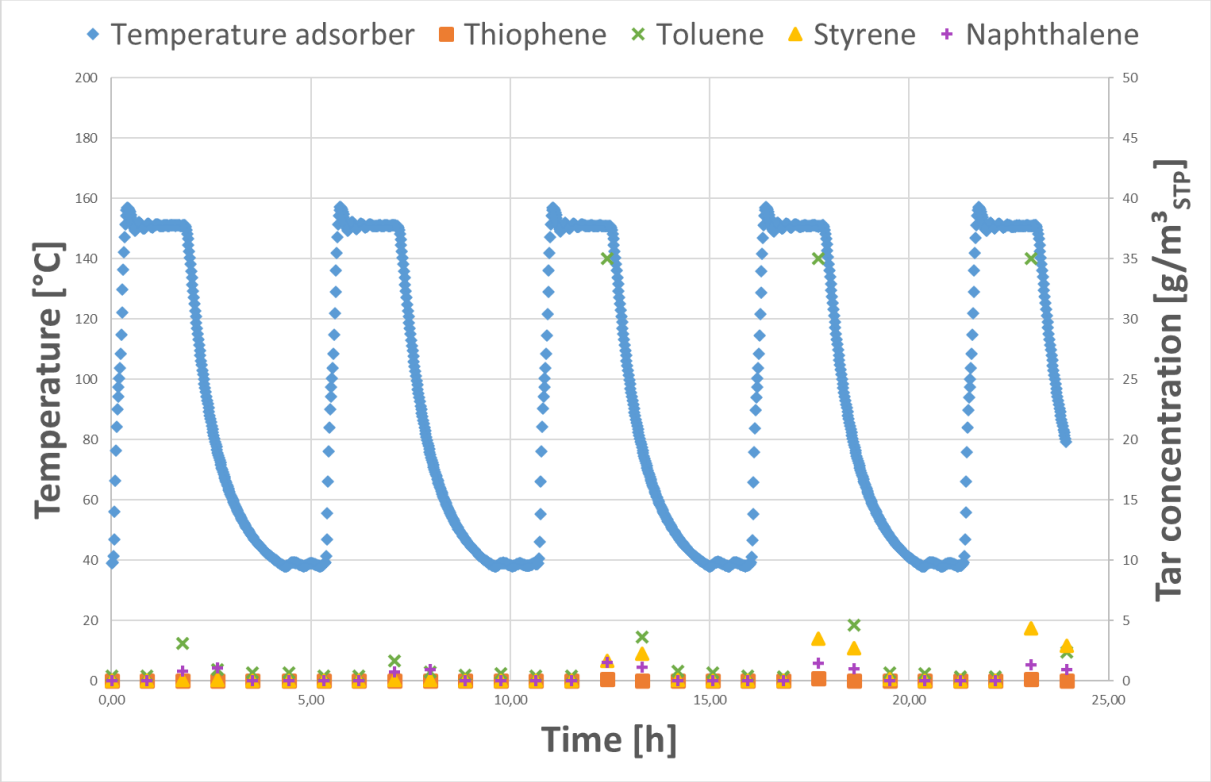

Figure 34: Trial 4, day 10. From the middle of the day, the values of all components increase; unfortunately, the reason for the previous drop is not clear.

The **fourteenth day** is similar to the tenth (see Fig. 34). Again, it is not possible to find out why the substances suddenly almost do not rise at all in the first two desorption phases and return to their usual course from the third onwards.

On the following two days the thiophene peaks increase more and more during desorption and finally reach a value of 2.3 g/m³. On the **seventeenth day** these vary enormously, namely between 1.1 and 24.4 g/m³. The styrene also increases on this day and reaches peaks around 5 g/m³.

The following day toluene shows peaks of only 12 to 20 g/m³. These, as well as the peaks of the other substances, occur at the same time, but in the range of the already decreasing temperature. Therefore, these irregularities may be due to a float of the GC system time. The next day gives unusual results. Thus, the peaks reappear in the usual places, but the substances give different results. The maximum values of thiophene vary between 2.5 and 7.2 g/m³. Naphthalene and styrene reach usual values, but over a longer period than usual. They are elevated at three measuring points in a row, i.e. for almost 2 hours each. This behaviour is still evident the next day.

The **days 21 to 23** provide constant results throughout, the only exception being the first two desorption phases. Here toluene reaches only 11.3 g/m³. The experiment was finally completed on 11.07.2019 at 20:48. The amount of activated carbon after weighing was 4.3393 g. The relatively high weight difference of 0.5793 g compared to the beginning could be due to the fact that the experiment was terminated at the

beginning of a desorption phase and the activated carbon was therefore still almost fully loaded.

The total tar concentration was between 1.5 and 2 during the desorption phases throughout the entire experiment, i.e. again lower than in the previous experiments. Fig. 35, which shows the twelfth day, serves as an example.

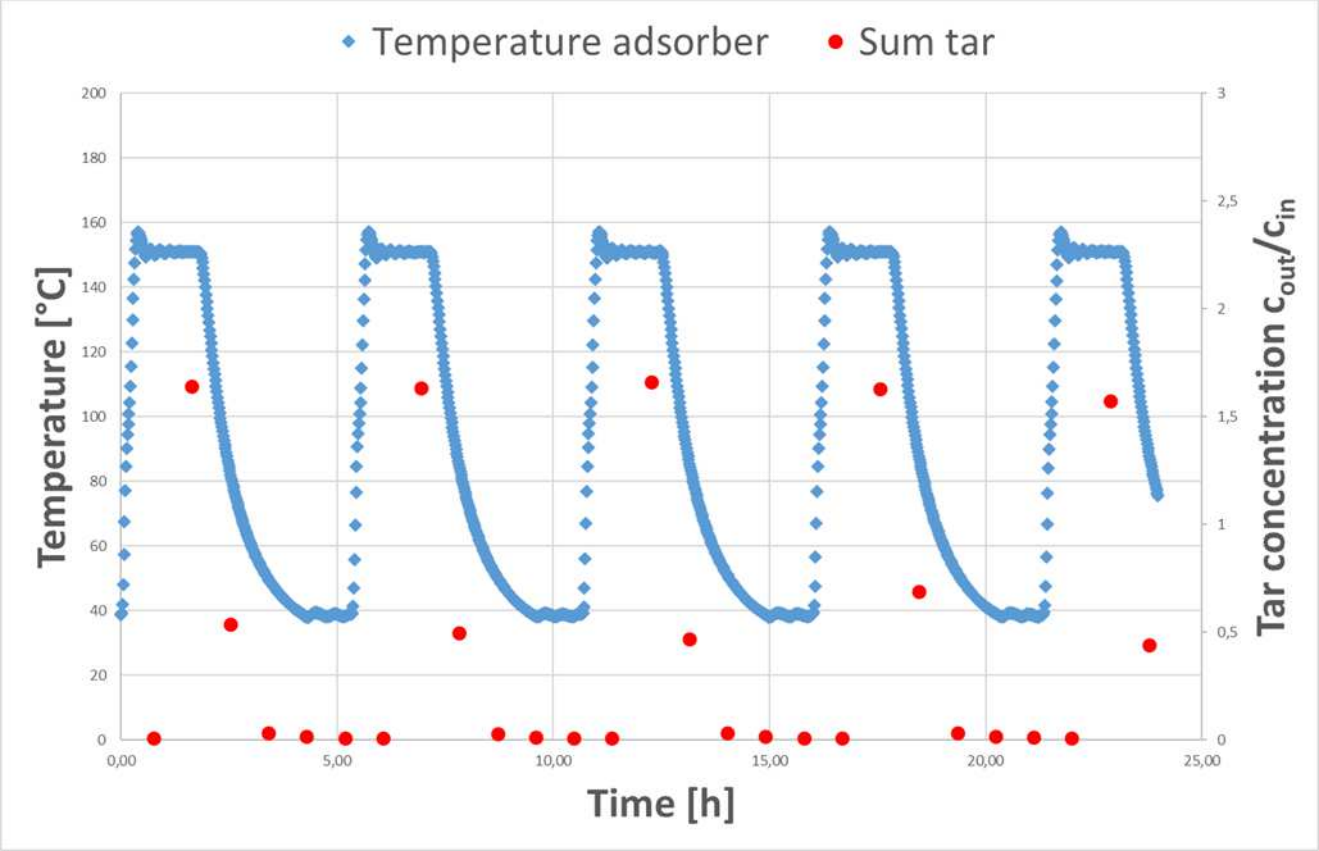

Figure 35: Exemplary overview of the tar concentration of this trial on day 12

The conclusion from this experiment is that in principle 152 °C is also sufficient to dissolve the tars from the activated carbon. However, this seems to increase the time until complete desorption of the substances, especially naphthalene, but also partly styrene. It was also found that thiophene and toluene are desorbed at least a little earlier than the other two substances.

4.1.5 Fifth trial

The fifth trial was started on 12.07.2019 at 08:37, the tars were detected for the first time at 09:08. The amount of activated carbon used was 3.76 g. As before, the duration of the individual phases is shown in Table 5. This time, a temperature of 180 °C was started directly. Thus, the individual components started with increased values right at the beginning. Toluene, which also reached its maximum during the other desorption phases of this day, came to a value of 35 g/m³. Styrene came to a quantity of 4.8 g/m³ and naphthalene to 3.6 g/m³. Thiophene only reached a value of 0.4 g/m³. Styrene also formed peaks during the following desorption phases, except for the second, but only in a range of 1.6 to 2 g/m³. In contrast, no further peak could be detected for

naphthalene during the entire first day. In the third desorption phase, a surprisingly high amount of thiophene was detected, namely 12.05 g/m³, which is also the absolute maximum of this substance during the fifth experiment. In general, it can be stated that the maximum values of the components occur relatively late during the individual desorption phases, i.e., as in experiment 2, they are slightly offset in time. This can be seen particularly well for toluene during the fourth and fifth desorption, see Fig. 36. This time offset continues throughout the entire experiment.

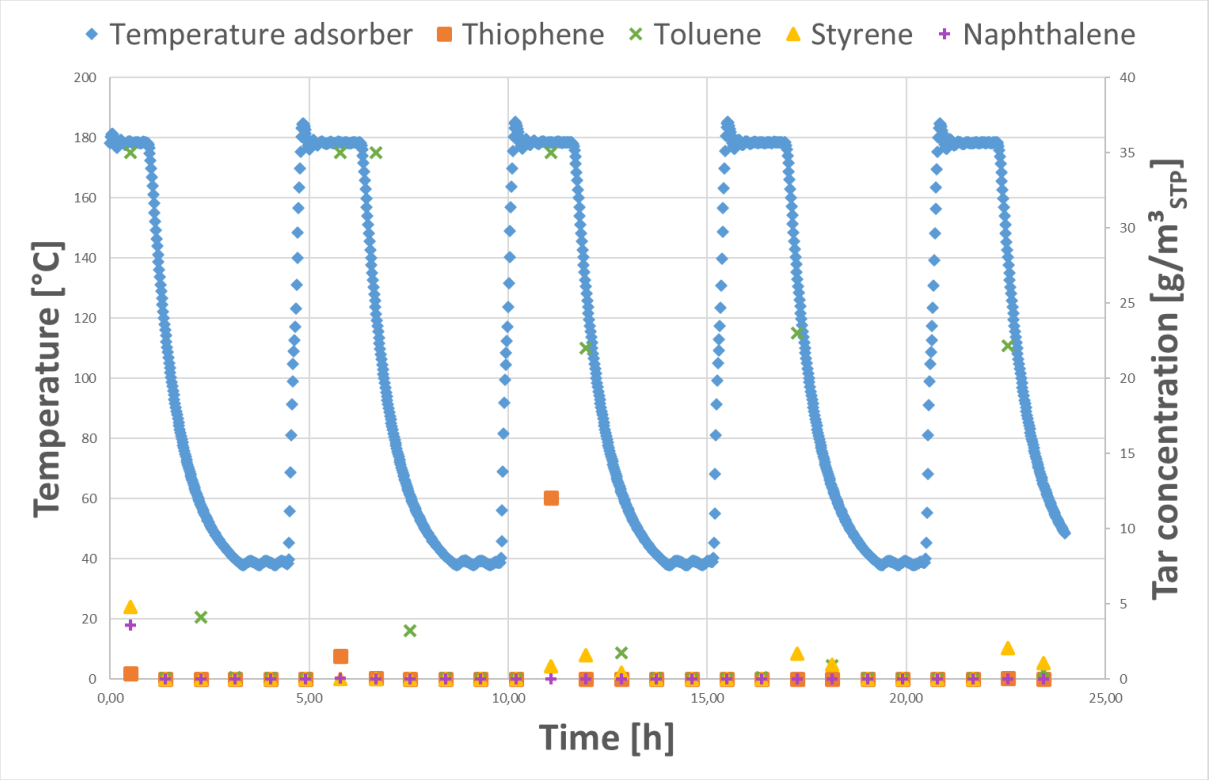

Figure 36: Fifth trial, day 1 with increasing thiophene values

During the **second day** it can be observed that the maximum values of toluene decrease more and more during desorption and finally are only 10 g/m³. In contrast, the peaks of styrene and naphthalene increase more and more and reach values of 7.4 and 2.5 g/m³, respectively. This could be due to the fact that the GC was not able to differentiate sufficiently between the individual components and thus partially incorrectly assigned them. On the **third day**, the values of toluene then increase again, but those of styrene and naphthalene do not decrease again, as would be expected according to the previous assumption. They reach maximum peaks of about 9 respectively 2.6 g/m³, see Fig. 37.

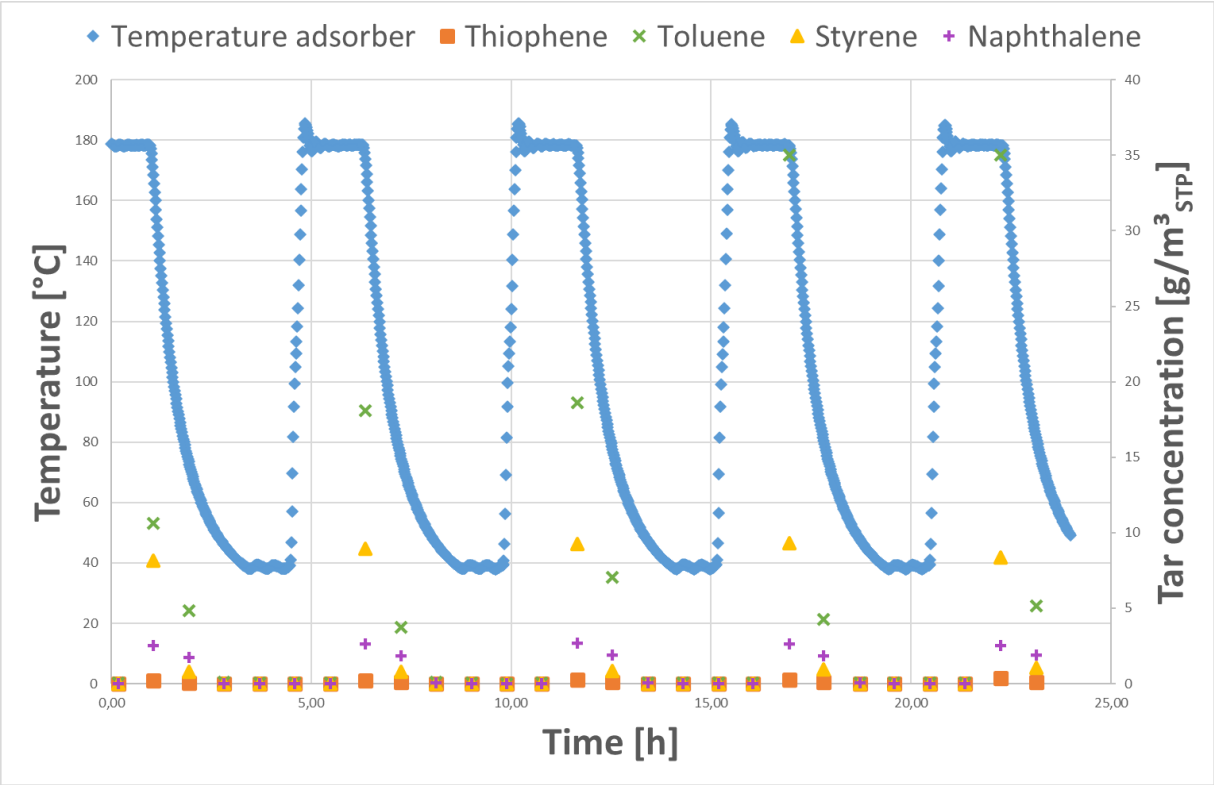

Figure 37: Fifth trial, day 3

The **fourth day** provides the most consistent results. During the desorption phases toluene reaches concentrations of 35 g/m³, styrene of about 6.5 g/m³, naphthalene of about 2.5 g/m³ and thiophene of 0.25 g/m³. Only during the last of these phases does styrene show a peak value of only 2.2 g/m³. At the beginning of the **fifth day** only naphthalene forms peaks. The other components are detected only very weakly, which unfortunately cannot be explained. Only after the third desorption phase does the usual picture return. This does not change on the **sixth day**, but a gradual increase of the thiophene values can be seen here, which culminates in a peak of 9.5 g/m³ during the third desorption. In the next one the usual picture is shown again, i.e. a value around 0.3 g/m³. Moreover, toluene also only forms a peak value of 2.5 g/m³.

During the desorption phase on **day seven** a constant behaviour for thiophene and naphthalene can be seen. Thus, peaks of approx. 0.25 g/m³ respectively approx. 2.5 g/m³ can be observed. Toluene and styrene initially only provide peak values of 5.5 g/m³ respectively 5 g/m³ but increase from phase to phase and reach values of 15.2 g/m³ respectively 7.8 g/m³ at the end of the day.

Days eight, nine and ten show throughout constant peaks of the individual components during the desorption phases. Thus, toluene generally reaches values of 35 g/m³, naphthalene is always in a range between 1.7 and 2.6 g/m³ and thiophene between 0.2 and 0.75 g/m³. Only styrene decreases in this period. Thus, the concentration of initially 8.1 g/m³ decreases and levels off between 1.9 and 2.9 g/m³ in days nine and ten. Fig. 38 shows as an example day 10.

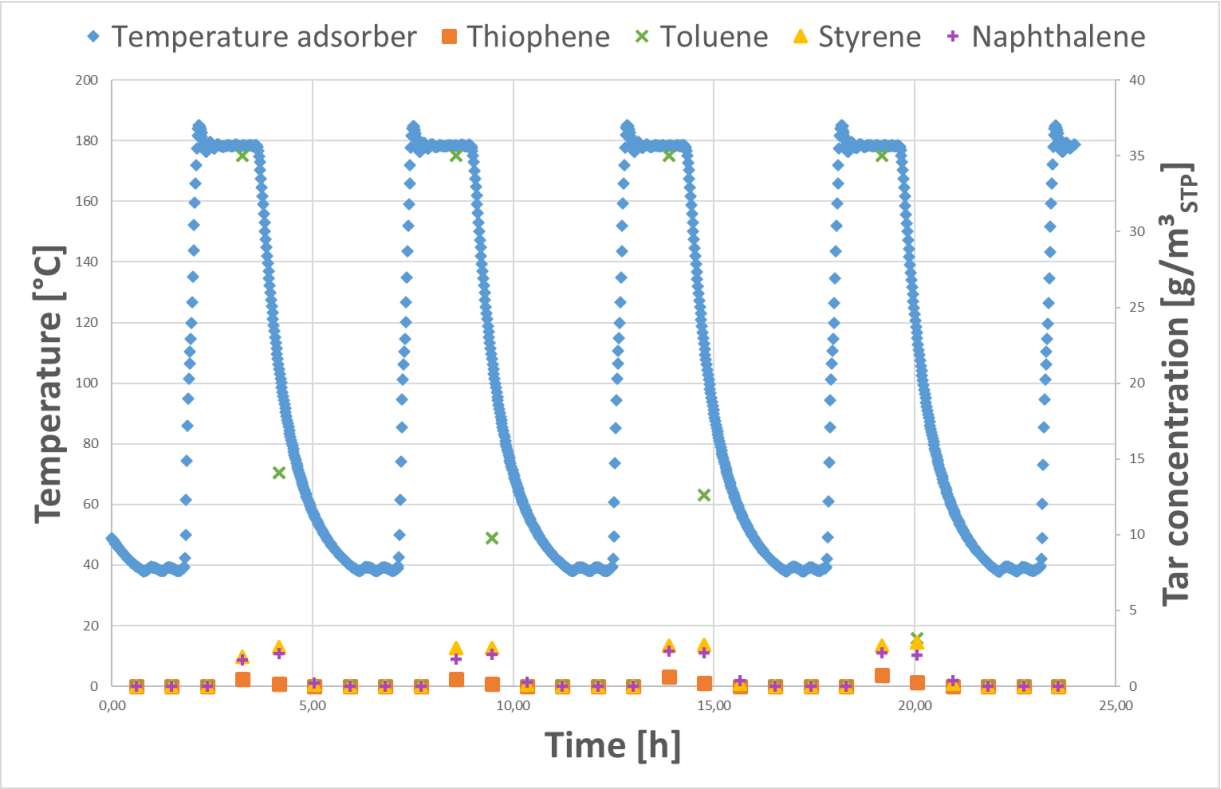

Figure 38: Fifth trial, day 10; throughout the whole day constant peaks

On the **eleventh** and thus last day, the desorption values of toluene decrease more and more, those of styrene and naphthalene remain largely constant and those of thiophene increase from the first to the third phase, from 1.4 via 2.5 to 8.3 g/m³, before returning to their usual level again from the fourth. It is interesting here that thiophene shows this behaviour on the first (see Fig. 36), sixth and eleventh day, i.e. every fifth day and always from the first to the third desorption.

In general, it can be said that toluene dissolves at maximum in the desorption phases for almost the entire duration of this experiment, reaching a value of 35 g/m³. Naphthalene also behaves constantly in these phases and always reaches values between 2 and 3 g/m³. The styrene, on the other hand, decreases over the entire period, with only a few deviations. Initially, 8 to 10 g/m³ are released during desorption, towards the end only 2 to 3 g/m³. The desorption values of thiophene, apart from the previously mentioned exceptions, are in the range of 0.2 to 0.7 g/m³. The mass of activated carbon after weighing was 4.1777 g. This means that at the end of this experiment, 0.4177 g of tar was still bundled in the activated carbon.

The tar concentration in this test is in about the same range as before. Seen over the entire course of the desorption phases, the tar concentration is usually between 1.4 and 1.8. Fig. 39, which shows day nine, serves as an example.

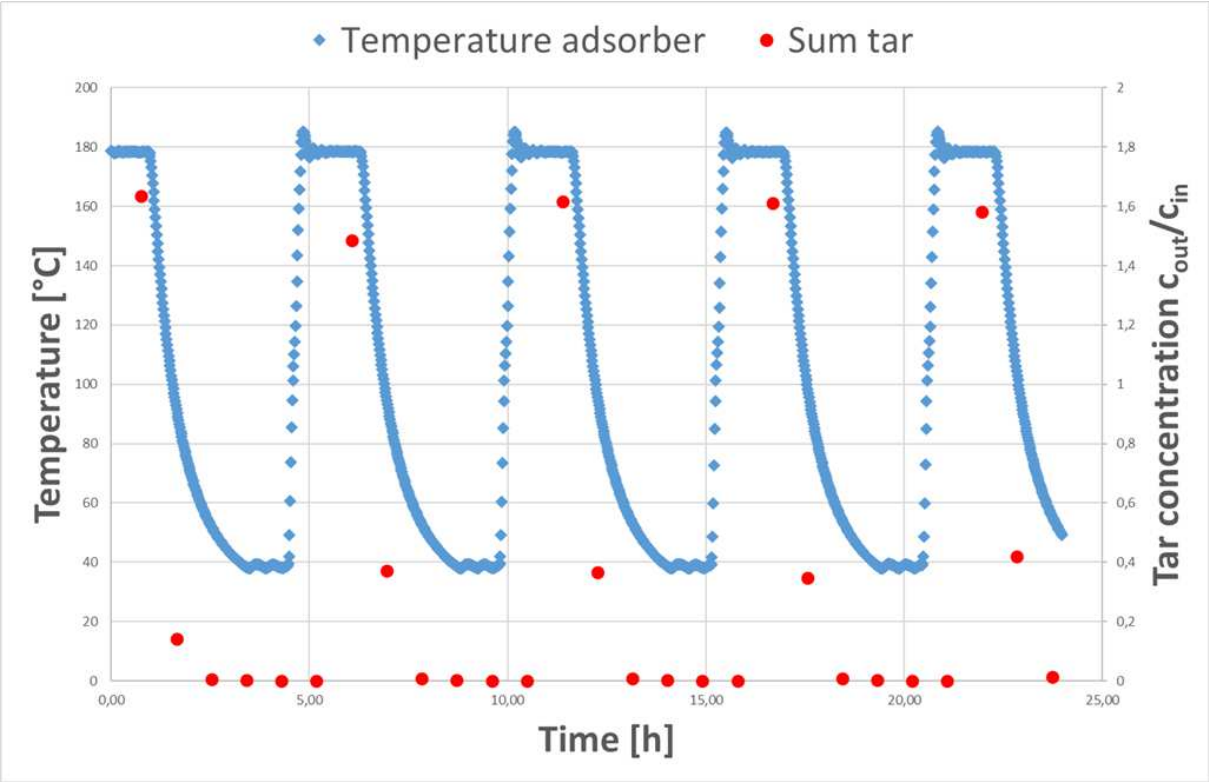

Figure 39: Exemplary overview of the tar concentration of the fifth trial on day 9

4.1.6 Sixth trial

The sixth and thus last trial was started on 23.07.2019 at 10:16, with the tars being detected for the first time one hour later. For this run 3.79 g of activated carbon were used. The duration of the individual phases as well as the amounts of gas were not changed this time either and can be seen in Table 5. The temperature for desorption was again set at 180 °C. In contrast to the previous experiments, however, hydrogen sulphide (H_2S) and carbonyl sulphide (COS) were added to the carrier gas. To be more precise it were 100 ppm H_2S and 10 ppm COS during adsorption.

It is only during the second desorption phase that components are released for the first time. However, only toluene in large amounts, namely again 35 g/m³, is detected. This value also represents the maximum value of toluene in this experiment and is reached at every desorption until the end of the third day. The other substances are below 0.1 g/m³. From the third desorption onwards, styrene and thiophene also form visible peaks. The styrene peaks reach values in the range of 2.3 to 3.6 g/m³ and the thiophene peaks are between 0.13 and 0.21 g/m³.

From the middle of the **second day**, naphthalene also forms peaks. These are at 1.4 g/m³ and are thus similar to those of styrene. The **third day** provides the most constant results. As mentioned before, toluene reaches 8 g/m³, styrene 1.4 to 1.8 g/m³, naphthalene 1.2 to 1.9 g/m³ and thiophene 0.08 to 0.54 g/m³. As in the previous trials, it can be seen that styrene and naphthalene form "wider" peaks, so take longer to desorb. Due to the shape of the peaks of these two substances, i.e. that the first is lower than the second at the two measuring points that show increased values, it can

also be concluded that these components are dissolved later than the other ones. Figure 40 shows this day.

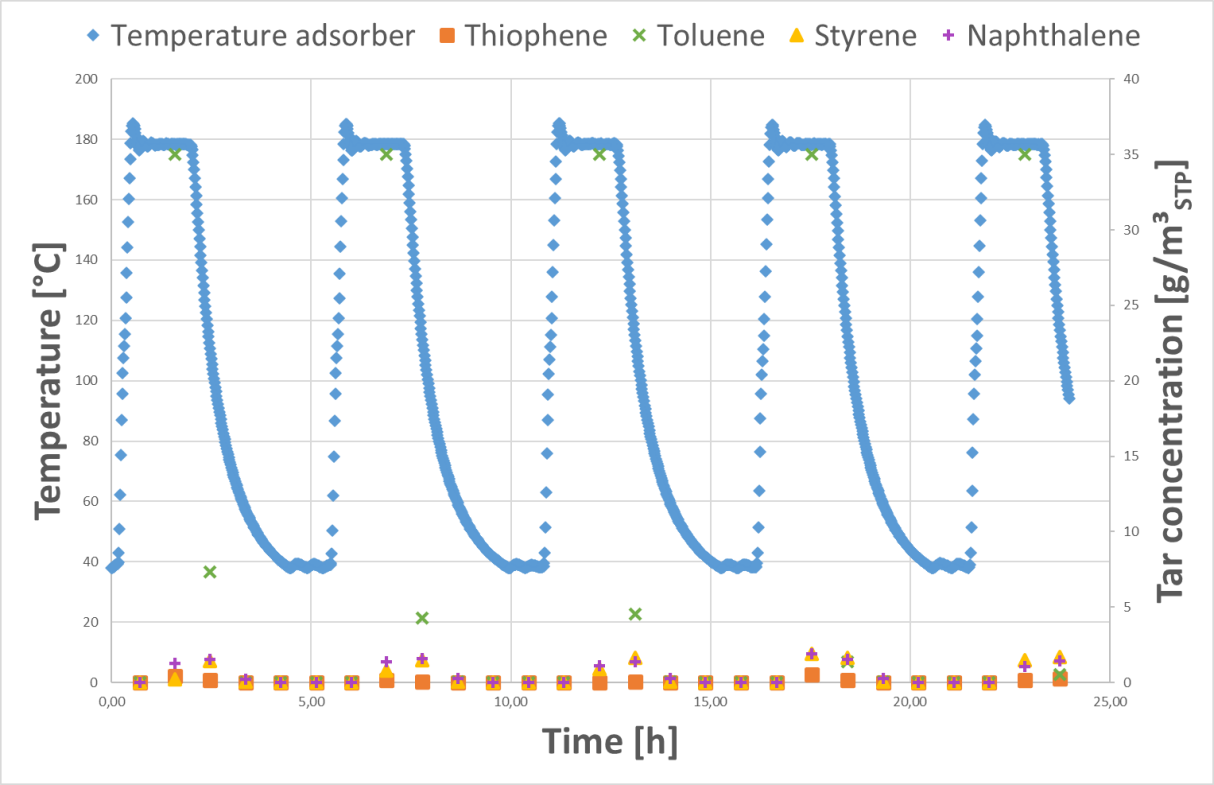

Figure 40: Sixth trial, day 3

From the **fourth day** on, the results are unfortunately no longer usable in a reasonable way, as they are determined by anomalies. The reason for this is probably the separation column, which has been severely damaged during the previous tests. Therefore, days four to ten will not be discussed further.

On 02.08.2019 at 09:33, after ten days, this trial was finally finished. The amount of activated carbon after weighing was 4.0548 g, which corresponds to a difference of 0.2648 g. As before, also this time the total tar concentration in the desorption phases, at least during the first three days, is approximately between 1.4 and 1.6. Fig. 41 shows the third day as an example.

It is difficult to gain any insights from this run, since more than half of the test days provide extremely atypical results. Whether this is related to the added components in the carrier gas can unfortunately not be answered after only one trial with it. However, the more likely reason for these irregularities could be that the previous tests had stressed the separation column so much that more precise measurements were not possible any longer.

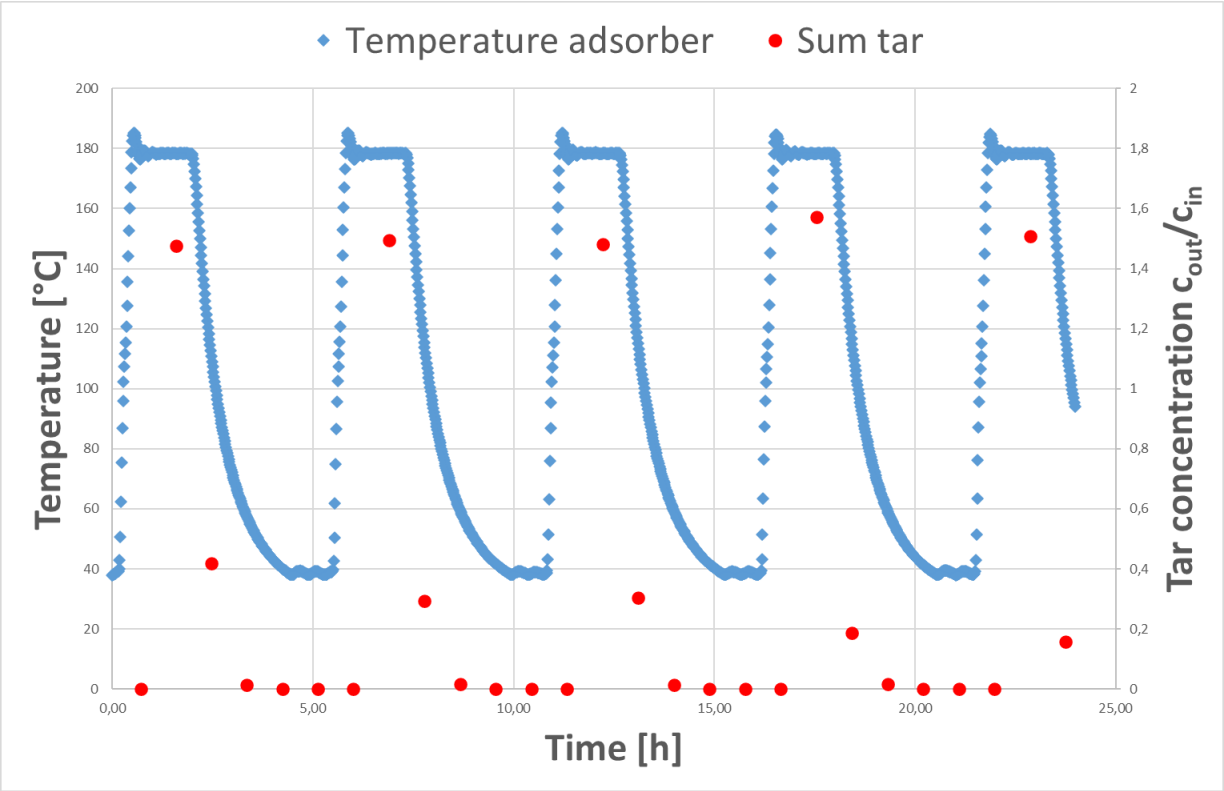

Figure 41: Sixth trial, day 3; example for the tar concentration in this trial

5. Summary and outlook

Tar residues resulting from biomass gasification represent a serious problem for the use of fuel gas in downstream applications, as they can contaminate and damage pipes and equipment. Similarly, sulphur compounds such as thiophene can lead to corrosion of pipes or poisoning of catalysts. In addition, tars also serve as a basic substance for various chemical products, so that further benefits can be derived from their removal. In our tests, activated carbon was used for tar removal.

Due to its high adsorption capacity and also its ability to take up volatile organic compounds, which are components of biomass tar, activated carbon is the most widely used adsorbent. It has also proven to be by far the most suitable adsorbent in tar removal studies compared to some other materials, such as low-cost wood chips and reusable synthetic porous cordierite. [43, 44]

After finishing all trials, the data was evaluated and interpreted. While the first three runs were primarily used to roughly determine the most suitable process parameters, only finer points were changed in tests 4 to 6. In addition, there were also some complications during the first half of the test series, for example the GC often failed. As a result, the data is only partially usable. Moreover, the results can only be interpreted conclusively to a limited extent due to the frequent changes in the influencing variables. The focus is thus on the second half of the test series.

However, there is one result from the second attempt that can be looked at more closely. The duration of the adsorption was first increased to 130 min and that of the subsequent desorption to 180 min. However, it was found that the substances were already released after half the time. From this it can be concluded that only about 70% of the adsorption time is needed to desorb the tar components. **After a 90 min loading phase, approx. 65 min would be sufficient for unloading.** In order to investigate this in more detail, further experiments with shorter measuring intervals would be helpful here.

During the course of the experiments it was found that during desorption thiophene and toluene were detected earlier, i.e. dissolved from the activated carbon, than the other two substances. This means that the separation over the adsorption cycles became worse. This is probably due to the thermal stress on the activated carbon caused by the hot/cold phases. The adsorption capacity of the activated carbon, however, was not affected by this. Due to the large intervals between the measurements, it is unfortunately not possible to say how much earlier or at what temperature exactly the substances are dissolved. This could also be determined more precisely by more frequent measurements, at least during the desorption phases, or by slowing down the heat-up phases.

As experiments on thiophene removal with activated carbon show, temperature plays the most important role in this process, along with flow rate. It was found that the adsorption capacity decreases with increasing temperature. Thus, it decreases by 80% with an increase from 100 °C to 150 °C and by a further 65% with a further increase to 200 °C. This decrease is due to the exothermic nature of the adsorption process. When applied to our experiments, this means that thiophene is still adsorbed to a small extent

if the desorption temperature is too low and therefore does not dissolve sufficiently. [44]

With regard to the temperature, **it was found that 152 °C is also sufficient to dissolve the tested substances from the activated carbon.** However, it was found that the desorption time of naphthalene and also styrene increased at least slightly. Since only one trial was carried out at this temperature, it cannot be said with certainty whether this was actually the case or whether it was due to an inaccuracy of the GC. Leaving aside possible complications in detection, it can be concluded that a higher temperature leads to faster desorption. Because a higher temperature is always combined with higher energy consumption, there is potential for savings. A series of tests at 170 °C, for example, would be conceivable. If this would only have a minor effect on the duration and completeness of the desorption, energy could be saved here.

To what extent the use of H_2S and COS in the carrier gas had an influence on the results is unfortunately difficult to say after a run with only three usable days. During these three days, however, it can be observed that toluene is maximally dissolved each time, while the other substances are weaker but very constant compared to the previous experiments. It is unfortunately not clear whether this is due to the components added to the carrier gas. Basically, one can assume that these additives have an influence. For example, experiments by Hanaoka *et al.* showed that in the presence of H_2S and COS, a massive increase in the breakthrough time could be observed during desulphurisation, although this was due to the addition of iron (Fe) to the activated carbon. This means that added iron contributes to the simultaneous removal of H_2S and COS. [45]

During the experiments some unusual events occurred which could be related to various complications and are briefly discussed here. For example, some unexpectedly high peaks may be due to the fact that the components in the tar syringe had separated after some time and the various substances had collected together. This could have led to an unusually high amount of a component being added and subsequently, of course, to increased detection. Similarly, this can also be the reason for unusually low values, i.e. when the accumulation of one substance has resulted in the injection of only a few parts of another substance. In further experiments this could be prevented by choosing a smaller syringe. Since the smaller volume means that less time passes until the substance is completely fed into the process, the mixture naturally has less time to separate.

Another explanation for some inconsistencies could be a separation column that is not suitable for this tar mixture. As a result, the GC could not sufficiently differentiate the components from each other, and atypical patterns of the substances occurred. Especially during the first 3 attempts this happened quite often and could be an explanation for it.

Generally, after the evaluation of the data, it can be said that further tests are necessary to obtain more precise results regarding the adsorption capacity/performance of activated carbon for tar removal. However, the evaluated data do provide promising results. It can therefore be assumed that the use of activated carbon also works outside the laboratory scale and can be used for the removal of tars. If one wants to break down the tar into its components, further tests are also necessary.

A slow increase in temperature should be considered in order to determine the solution temperatures of the individual substances. The successful separation of these substances could further contribute to the independence of the chemical industry from fossil raw materials.

6. Nomenclature

ΔH…standard enthalpy [kJ/mol]

b…Langmuir constant [-]

c_i…concentration of the adsorbate at the inlet [g/m^3]

c_o…concentration of the adsorbate at the outlet [g/m^3]

k…Freundlich constant [-]

k_H…Henry constant [-]

n…Freundlich exponent [-]

p_A…partial pressure [Pa]

p_{tot}…total pressure [Pa]

t_b…breakthrough time [h]

t_h…half-life [h]

t_s…time to complete saturation [h]

X…loading of adsorbent [kg/kg]

X_m…maximum possible monomolecular loading [kg/kg]

7. List of Figures

8. List of Tables

9. List of References

[1] Frischenschlager, H.; et al.: (6/2018) Roadmap 2050 Biobasierter Kunststoff, Abgerufen von: https://nachhaltigwirtschaften.at/de/publikationen/schriftenreihe-2018-06-bbks-szenario.php [29.11.2019]

[2] Gruß, A.: (2018, 4.Oktober) Chemie ohne Erdöl?, Abgerufen von: https://www.chemanager-online.com/themen/strategie/chemie-ohne-erdoel [16.11.2019]

[3] Wagner, S.; et al.: Nachwachsende Rohstoffe für die chemische Industrie, Abgerufen von: https://nachhaltigwirtschaften.at/, Bundesministerium für Verkehr, Innovation und Technologie, Wien, 2005

[4] Pietzsch, J.: Bioökonomie für Einsteiger, Springer-Verlag, Berlin, 2017

[5] Kamm, B.: Produktion von Plattformchemikalien und Synthesegas aus Biomasse, Wiley-VCH, Weinheim, 2007

[6] Loipersböck, J; et al.: Developing an adsorption-based gas cleaning system for a dual fluidized bed gasification process, 2019

[7] Bardolf, R.: Optimierung eines Produktgaswäschers bei der Biomassedampfvergasung im Zweibettwirbelschichtverfahren, Dissertation, TU Wien, 2017

[8] Wesselak, V.; et al.: Handbuch Regenerative Energietechnik, Springer Vieweg, Berlin, 2017

[9] Kaltschmitt, M.; et al.: Energie aus Biomasse, Springer-Verlag, Berlin, 2009

[10] Arpe, H.-J.: Industrielle organische Chemie, Wiley-VCH Verlag, Weinheim, 2007

[11] https://www.spektrum.de/lexikon/chemie/synthesegas/8953 [03.12.2019]

[12] Wiemann, S.: Erzeugung und Verwendung von Synthesegas in Verbrennungsmotoren, Uni Duisburg-Essen, 2018, Dissertation

[13] Reil, S.: Zur Biomassevergasung in „stratified downdraft“ Reaktoren und deren Prozessstabilisierung, Erlangen-Nürnberg, 2019, Dissertation

[14] Neubauer, Y.: Online-Analyse von Teer aus der Biomassevergasung mit Lasermassenspektroskopie, Berlin, 2008, Dissertation

[15] Milne, T.A.; Evans, R.J.: Biomass Gasifier “Tars”: Their Nature, Formation and Conversion, National Renewable Energy Laboratory NREL, Golden, Colorado, 1998, Forschungsbericht

[16] Greim, H.: The MAK-Collection for Occupational Health and Safety, Wiley-VCH, 2002

[17] https://www.chemie.de/lexikon/ [24.05.2019]

[18] https://roempp.thieme.de/lexicon/ [17.10.2019]

[19] Niziolek, A. M.; et al.: Biomass Based Production of Benzene, Toluene, and Xylenes via Methanol: Process Synthesis and Deterministic Global Optimization; Department of Chemical and Biological Engineering, Princeton University, Princeton, New Jersey 08544, United States

[20] https://ihsmarkit.com/products/benzene-chemical-economics-handbook.html [16.01.2020]

[21] “Aktualisierte VCI-Analyse zur Basischemie 2030“, Verband der Chemischen Industrie e.V., Frankfurt am Main, 2016

[22] https://www.ikb-blog.de/rohstoffpreise/ [16.01.2020]

[23] https://www.penpet.de/news [16.01.2020]

[24] https://www.ceresana.com/de/marktstudien/chemikalien/styrol/ [17.01.2020]

[25] https://www.kiweb.de [29.05.2019]

[26] https://oxxynova.com/de/home/de/ [17.01.2020]

[27] The Future of Petrochemicals: Towards more sustainable plastics and fertilisers, OECD/IEA, 2018

[28] „Quartalsbericht 1.2020“, Verband der Chemischen Industrie e.V., Frankfurt am Main, 2020

[29] Bandi, A.: Verfahrensübersicht: Gasreinigungsverfahren, FVS Fachtagung 2003, retrieved from: https://www.fvee.de/ [22.12.2019]

[30] Bolhar-Nordenkampf, M.; Jörg, K.: Gasreinigung – Stand der Technik, Institut für Verfahrenstechnik, TU Wien, 2003

[31] Böhning, D.; Beckmann, M.: Dezentrale Biomassevergasung – Teerabbau durch primäre und sekundäre Maßnahmen. In: Thomé-Kozmiensky, K.J.; Beckmann, M.: Erneuerbare Energien – Band 2., TK Verlag Thomé-Kozmiensky, Neuruppin, 2009

[32] Schmidt, E.: Gasreinigung, Chemie Ingenieur Technik, Wiley-VCH, Weinheim, 2007

[33] Kast, W.: Adsorption aus der Gasphase, VCH Verlagsgesellschaft, Weinheim, 1988

[34] Bathen, D.; Breitbach, M.: Adsorptionstechnik, Springer Verlag, 2001

[35] Sattler, K.: Thermische Trennverfahren, VCH Verlagsgesellschaft, Weinheim, 1988

[36] Mersmann, A.; et al.: Abtrennung und Rückgewinnung von gasförmigen Stoffen durch Adsorption. Chemie Ingenieur Technik 63(9): 892–903, 1991

[37] Mersmann, A.: Thermische Verfahrenstechnik, Springer Verlag, 1980

[38] Reschetilowski, W.: Technisch-Chemisches Praktikum, Wiley VCH Verlag, Weinheim, 2002

[39] Patat, F.; Kirchner, K.: Praktikum der Technischen Chemie, Walter de Gruyter& Co., Berlin, 1963

[40] https://donau-carbon.com/Downloads/aktivkohle.aspx [24.10.2019]

[41] Schomburg, G.: Gaschromatographie, VCH Verlagsgesellschaft, Weinheim, 1987

[42] Gressner, A. M.; Arndt, T.: Lexikon der Medizinischen Laboratoriumsdiagnostik, Springer Verlag, Berlin, 2013

[43] Phuphuakrat, T.; et al.: Tar removal from biomass pyrolysis gas in two step function of decomposition and adsorption, Elsevier Ltd., 2009

[44] Edinger, P.; et al.: Adsorption of thiophene by activated carbon: A global sensitivity analysis, Journal of Environmental Chemical Engineering, 2017

[45] Hanoaka, T.; et al.: Hot and Dry Cleaning of Biomass Gasified Gas Using Activated Carbons with Simultanous Removal of Tar, Particles, and Sulfur Compounds, MDPI, Basel, 2012